AFRL-SR-AR-TR-04-

0095

REPORT DOCUMENTATION PAGE

1. REPORT DATE (DD-MM-YYYY)	2. REPORT TYPE	3. DATES COVERED (From - To)
20-01-2004	STTR Phase I Final	15 Aug 2002 – 20 Jan 2004

4. TITLE AND SUBTITLE
Nanomodified Carbon/Carbon Composites for Intermediate Temperature

5a. CONTRACT NUMBER
F49620-02-C-0086

5b. GRANT NUMBER

5c. PROGRAM ELEMENT NUMBER

6. AUTHOR(S)
1. Koo, J. H.
2. Pilato, L. A.
3. Pittman, Jr., C. U.
4. Winzek, P.

5d. PROJECT NUMBER

5e. TASK NUMBER

5f. WORK UNIT NUMBER

7. PERFORMING ORGANIZATION NAME(S) AND ADDRESS(ES)

1. University of Texas at Austin, Dept. of Mechanical Engineering, 1 University Station, C2200, Austin, TX 78712-0292

2. Pilato Consulting
598 Watchung Road, Bound Brook, NJ 08805

3. Mississippi State University
UICRC, Box 9573, Mississippi State, MS 39762

8. PERFORMING ORGANIZATION REPORT NUMBER
4. HITCO Carbon Composites
1600 West 135th St., Gardena, CA 90249

9. SPONSORING / MONITORING AGENCY NAME(S) AND ADDRESS(ES)
Dr. Charles Y-C Lee
AFOSR/NL
4015 Wilson Blvd., Room 713
Arlington, VA 22203-1954

10. SPONSOR/MONITOR'S ACRONYM(S)
AFOSR

11. SPONSOR/MONITOR'S REPORT NUMBER(S)

12. DISTRIBUTION / AVAILABILITY STATEMENT

Approved for public release; distribution unlimited

20040213 119

13. SUPPLEMENTARY NOTES

14. ABSTRACT An improved Carbon/Carbon Composite (CCC) with enhanced thermo-oxidative resistant performance at intermediate temperatures (700 to 1200° F) was investigated. A nanophase was introduced into the CCC (NCCC) prior to cure for improved and maintained mechanical strength by preventing oxidation of the composites. Three types of nanoparticles: chemically modified MMT clay, POSS®, and carbon nanofiber (CNF), were used in conjunction with precursor resins such as cyanate ester (CE) and baseline phenolic resole. Six resin/nanoparticle material systems were selected and transformed into prepregs, followed by fabrication into composites for carbonization and densification to produce CCC. Heat aging of the CCCs was conducted for 24 hours at 700 and 1200° F in N_2 for the six candidates and baseline commercial CCC material, followed by heated air for 8 hours (simulated thermo-oxidative conditions). TEM analyses indicate nanoparticles were more uniformly dispersed in CE than in the baseline phenolic resole. Higher room temperature ultimate tensile strength and modulus values and better thermo-oxidative resistance for nanomodified CE materials in comparison to both baseline and nanomodified phenolic resole materials are presented as evidence for nanophase presence in the CE based nano CCC materials. CE based NCCC exhibited higher density than baseline CCC and phenolic resole based NCCCs. Carbon nanofiber modified CE had the highest strength and showed the largest maximum failure load (both at RT and 1200° F) and gradually fell off to 75% until complete failure. The CNF nanophase provided enhanced ductility as well as increasing the ultimate strength - further evidence of increased thermal resistance of the nanophase.

15. SUBJECT TERMS STTR Phase I Report, Carbon Carbon Composite, Thermo-oxidative Resistance, Nanophase, Surface Modified MMT Clay, POSS®, Carbon Nanofiber, Cyanate Esters, Phenolic Resole, TEM, WAXD, Interlaminar Shear Strength, Carbonization, Densification, Ductility, Tensile Strength, Elastic Modulus, Poisson's Ratio.

16. SECURITY CLASSIFICATION OF:			17. LIMITATION OF ABSTRACT	18. NUMBER OF PAGES	19a. NAME OF RESPONSIBLE PERSON
a. REPORT	b. ABSTRACT	c. THIS PAGE			Joseph H. Koo
U	U	U	U	36	19b. TELEPHONE NUMBER (Include area code) (512) 589-4170

NANOMODIFIED CARBON/CARBON COMPOSITES FOR INTERMEDIATE TEMPERATURE

Air Force Office of Scientific Research (AFOSR)
Contract No. F49620-02-C-0086 (STTR Phase I)

Submitted to

Dr. Charles Y-C Lee
AFOSR/NL
4015 Wilson Blvd, Room 713
Arlington, VA 22203-1954

January 20, 2004

Prepared by

J.H. Koo[1*], L.A. Pilato[2], C.U. Pittman, Jr.[3], and P. Winzek[4]

[1]The University of Texas University at Austin, Dept. of Mechanical Engineering, 1 University Station, C2200, Austin, TX 78712-0292

[2]Pilato Consulting, 598 Watchung Rd., Bound Brook, NJ 08805

[3]Mississippi State University, UICRC, Box 9573, Mississippi State, MS 39762

[4]HITCO Carbon Composites Inc., 1600 West 135th St., Gardena, CA 90249

[*]Corresponding author: jkoo@mail.utexas.edu

NANOMODIFIED CARBON/CARBON COMPOSITES FOR INTERMEDIATE TEMPERATURE

Air Force Office of Scientific Research (AFOSR)
Contract No. F49620-02-C-0086 (STTR Phase I)

Submitted to

Dr. Charles Y-C Lee
AFOSR/NL
4015 Wilson Blvd, Room 713
Arlington, VA 22203-1954

January 20, 2004

Prepared by

J.H. Koo[1*], L.A. Pilato[2], C.U. Pittman, Jr.[3], and P. Winzek[4]

[1]The University of Texas University at Austin, Dept. of Mechanical Engineering, 1 University Station, C2200, Austin, TX 78712-0292

[2]Pilato Consulting, 598 Watchung Rd., Bound Brook, NJ 08805

[3]Mississippi State University, UICRC, Box 9573, Mississippi State, MS 39762

[4]HITCO Carbon Composites Inc., 1600 West 135th St., Gardena, CA 90249

[*]Corresponding author: jkoo@mail.utexas.edu

TABLE OF CONTENTS

EXCUTIVE SUMMARY

The major objective of this material program is to develop an improved carbon/carbon (C/C) composite with enhanced thermo-oxidative resistant performance at intermediate temperatures (700° to 1,200°F). We proposed that a nanophase be introduced into the C/C composites (CCC), prior to cure, to provide improved and maintained mechanical strength by preventing oxidation of the composites. In this study, we used three resin systems: Lonza low and medium viscosity cyanate esters (CE), PT-15 and PT-30, and Hitco phenolic, 134A; and three types of nanoparticles: chemically modified montmorillonite (MMT) organoclays, polyhedral oligomeric silsesquioxanes (POSS®), and carbon nanofibers (CNF) to create new types of CCC. Wide angle X-ray diffraction (WAXD) and transmission electron microscopy (TEM) were used to determine the degree of dispersion.

Six resin/nanoparticle material systems were selected to produce prepregs at Hitco. The prepregs were fabricated into composites for carbonization and densification to produce CCC. A set of four 12.25- by 12.25- by 0.15-inch CCC panels were fabricated for all the CCCs for physical, thermal, and mechanical properties characterization. Heats aging of CCCs were conducted for 24 hrs at 700° and 1,200° F in nitrogen for the six candidates and the baseline Hitco CC139 materials. These materials were then exposed to heated-air for 8 hrs to simulate thermo-oxidative conditions. Mechanical properties such as tensile strength and modulus, Poisson's ratio, and interlaminar shear strength were determined on the C/C nanocomposites and compared with the baseline CCC.

The TEM analyses indicated that the MMT clay, POSS®, and CNF nanoparticles dispersed very well in the cyanate ester resins and not as well in the phenolic resin. Evidence is presented that a nanophase is formed when nanoparticles such as surface treated clay, carbon nanofibers or POSS® are introduced into cyanate ester as well as phenolic resins. Higher room temperature ultimate tensile strength and modulus values for the nanomodified materials are presented as evidence for nanophase presence in the CE or phenolic resin systems as compared to lower strength/modulus for the phenolic resin control. Thermo-oxidative studies indicated that the cyanate ester-based nanomodified CCCs (NCCC) were more thermo-oxidative resistant than the phenolic-based standard baseline CCC. The phenolic-based NCCCs were not as thermo-oxidative resistant than the standard baseline CCC. The cyanate ester-based NCCCs have higher density than the baseline CCC and the phenolic-based NCCCs. A trend of higher density NCCCs exhibiting in better thermo-oxidative resistant NCCC was proposed.

Higher ultimate tensile strength and elastic modulus values were obtained for NCCCs as compared to baseline CCC CC139. Interlaminar shear strength (ILSS) of NCCCs and baseline CC139 were similar. Carbon nanofiber modified cyanate ester had the highest strength and exhibited the largest maximum failure load (both room temperature and 1,200° F) and gradually fell off to 75% until complete fracture. The CNF nanphase provided enhanced ductility while increasing the ultimate strength -- further evidence of increased thermal resistance of the nanophase.

1.0 INTRODUCTION

Carbon/carbon (C/C) structures are traditionally designed and optimized for high temperature applications. They have very high temperature capabilities under inert atmospheric conditions, but without oxidation protection, they suffer from thermo-oxidative instability above ~700°F and result in poor mechanical strength. Oxidation protection technologies developed to be used above ~1800°F in thermo-oxidative environments have had limited success. Carbon/carbon composites (CCC) would be ideal materials to extend organic-based material systems beyond the 700°F limit if their mechanical strength can be improved and maintained by preventing oxidation of the composite.

The major objective of this material program is to develop a better CCC with enhanced thermo-oxidative resistant performance at intermediate temperatures (700° to 1,200°F). We proposed that a nanophase be introduced into the CCC, prior to cure, to provide improved and maintained mechanical strength by preventing oxidation of the composites. In this study, we used (a) *three resin systems*: Lonza low and medium viscosity cyanate esters, PT-15 and PT-30, and Hitco phenolic, 134A; (b) *three types of nanoparticles*: chemically modified montmorillonite (MMT) organoclays, polyhedral oligomeric silsesquioxanes (POSS®), and carbon nanofibers (CNF) to create new types of CCC.

The minor objectives of this investigation are to: (a) develop processes to disperse these nanoparticles uniformly in the cyanate esters and the phenolic resin prior to curing, (b) use wide-angle X-ray diffraction (WAXD), transmission electron microscopy (TEM), and scanning electron microscopy (SEM) to characterize polymer nanocomposite structures after curing, (c) study structure-property relationship of these types of new materials, and (d) evaluate the performance (mechanical properties) of these materials in the intermediate temperature range (700° – 1,200°F) after carbonization.

Six resin/nanoparticle material systems were selected to produce prepregs at Hitco Carbon Composites. The prepregs were fabricated into composites for carbonization and densification to produce C/C composites. Heat aging of CCCs was conducted for 24 hrs at 700° and 1,200°F for the six candidates and the baseline Hitco CC139 materials. Mechanical properties such as the tensile strength and modulus, and interlaminar shear strength were determined on the C/C nanomaterials and are compared with the baseline CCC.

2. SELECTION OF MATERIALS

2.1 Resin Systems Three resin systems were selected for this study, they are Lonza's Primaset® PT-15 and PT-30 cyanate esters and Hitco's 134A phenolic resin system.

Cyanate Ester Resin The polymer system is the most important component of the CCC materials. Lonza Corporation's Primaset® PT-30 multifunctional cyanate ester was selected for this study. This matrix has 65% char yield, less than 0.5% volatiles, and no decomposition by-products during curing, and low viscosity (80cP) at 120°C. The chemical structure of PT-30 resin is shown in Figure 1. Shivakumar *et al.* [1, 2] used this resin for the fabrication of CCC successfully. PT-15 is a multifunctional, low viscosity liquid cyanate ester resin, similar to PT-30.

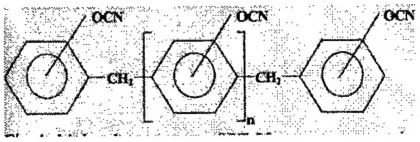

Figure 1 Molecular structure of PT-30 cyanate ester resin

Phenolic Resin The Hitco-specific resin, 134A [3], a resole amine-containing phenolic was used as the baseline resin material. The resin is a phenol-formaldehyde system made specifically for Hitco, but is similar in many ways to another commercial phenol-formaldehyde resin such as Borden Chemical SC-1008. The main properties relevant to the formation of a carbon/carbon composite are its char yield and the type of crack structure generated to be favorable to infiltration during the chemical vapor infiltration (CVI) process.

Hitco CC139 material (baseline CCC for this study) is a standard commercial material that has been manufactured by Hitco for a number of applications for several years. Its basic construction is a PAN fiber fabric lay-up with a Hitco-specific phenolic resin (134A), carbonized and processed using CVI to a density of 1.75 g/cc. The 134A resin is mixed with a fill material of carbon black to help tailor the shrinkage and porosity for the CVI. Typical physical properties for a 0/90 lay-up pattern are given in Table 1 [4].

Table 1 Physical Properties of Hitco CC139

PROPERTY	**VALUES**
Density, g/cc	1.75
CTE in plane, ppm/°C	0.7
CTE through thickness, ppm/°C	8.8
TC in-plane, W/m-K	34
TC through thickness, W/m-K	9.3
Tensile strength, ksi	50
Tensile modulus, msi	16
Compressive strength, ksi	30
Compressive modulus, msi	14
Flexural strength, ksi	44
Flexural modulus, msi	15
Shear strength, ksi	5.0
Shear modulus, msi	0.8
Notched Izod impact, fppi	13
Beam shear (4:1), ksi	2.7
Crossply tension, ksi	1.2

2.2 Polymer Nanoparticles Three types of nanoparticles were used in this study, namely Southern Clay Products' montmorillonite (MMT) nanoclays, Hybrid Plastics' Polyhedral Oligomeric Silsesquioxanes (POSS®) materials, and Applied Sciences' carbon nanofibers (CNF). These nanoparticles will reinforce the polymer in the nanoscale and will enhance the dimensional stability and mechanical properties of the polymer nanocomposites. To achieve the potential improvements it usually requires some degree of exfoliation and dispersion. These are shown to be dependent upon a combination of proper chemical treatment and optimized processing.

Nanoclays Six MMT nanoclays including Southern Clay Products (a) Cloisite® 10A (a natural MMT modified with a quaternary ammonium salt), (b) Cloisite® 30B (a natural MMT modified with a ternary ammonium salt) and (c) Cloisite® Na^+ (a natural MMT); Nanocor (d) Nanomer®

I.28E (an onium ion surface modified MMT mineral), (e) Nanomer® I.30E (an onium ion surface modified MMT mineral), and (f) PGW (Na^+, no organic pillaring) were selected.

POSS® The lab scale dispersion of these materials has involved the examination of seven POSS® chemicals including (a) trisilanol phenyl POSS® (SO1458), (b) cyanopropyl cyclopentyl POSS® (NI0910), (c) a tetra-β-substituted styryl POSS® with four epoxy groups [POSS(1)], (d) epoxy cyclohexyl dimethylsilyl POSS®, (e) octaisobutyl POSS®, (f) poly(phenyl silsesquioxane) (PPSQ) (PM1270), and (g) dichloromethylsilylethyl isobutyl POSS® (CS0335) to prepare nanocomposites.

CNF Two Applied Sciences Pyrograf® III carbon nanofibers (CNF) (a) PR-19-PS (128 nm in diameter) and (b) PR-24-PS (65 nm in diameter) were selected in this study.

The TEM analyses were conducted on selective specimens. These TEM images facilitated screening various formulations for desirable nano-level dispersion of the clay or POSS® or CNF within the cure resin/inorganic composites. Desirable features included higher levels of clay exfoliation, molecular dispersion of POSS®, and uniform dispersion of CNF within the resin both before and after curing.

3. DISCUSSION OF RESULTS

The candidate materials developed are screened for dispersion using WAXD and TEM prior to full scale up. Lab scale dispersion of (a) PT-30 with different wt% POSS®, nanoclays, and CNF, (b) PT-15 with different wt% of POSS® and nanoclays, and (c) 134A with different wt% POSS® and nanoclays were conducted. The morphology of selective resin/nanoparticle systems were characterized using TEM and SEM analyses.

3.1 Processing and Characterization of PT-30/Nanoparticle Systems Weight percent (wt%) of (99/1), (97/3), and (90/10) of seven POSS® chemicals were blended with PT-30 for a total of 15 blends using a lab scale high shear mixer. Appearance in terms of transparency, translucency, or opaqueness was examined during mixing, before and after curing for all blends and densities were recorded. Based on visual observations trisilanol phenyl POSS® is the only potential POSS® compound that works well with PT-30 using direct melt blending process. All other blends were either opaque or translucent and particles were observed. Phase separation had clearly taken place. Selective candidates were cured for TEM analyses.

PT-30 curing with three catalysts: (a) copper (II) acetylacetonate ($(Cu/AcAc)_2$), manganese (III) acetylacetonate ($Mn(AcAc)_3$), and cobalt (III) acetylacetonate ($Co(AcAc)_3$) were used for PT-30 curing studies. It was demonstrated that a phenolic promoter was needed for these catalysts to be fully effective. Further metal salts are undesirable and deleterious to the thermal oxidative resistance of CCC. As a result, no catalyst was used in the remainder of this study. PT-15 and PT-30 were cured thermally. They can be readily handled at 110°C without much change in viscosity. At this temperature they have low viscosities, and nanoparticles are readily introduced by stirring or high shear blending. PT-15 is held at 110°C for 30 min., then 188°C for 2 hr, then 200°C for 10 min. followed by raising the temperature 10°C every 5 min. until reaching 250°C where it was held for 2.75 hr. Similar protocols are used with PT-30.

PT-30/Cloisite® 10A (98/2) was cured, and phase separation were observed. PT-30/Cloisite® 30B blended in THF (97.5/2.5) and (96.5/3.5) were cured, resulting in the preparation of a total

of 3 blends. THF is removed in vacuum prior to curing. PT-30/PR-19-PS and PT-30/PR-24-PS were blended in (99.5/0.5) and (99/1) wt% and a total of 4 CNF blends were prepared.

Cloisite® 30B was first dispersed in THF before blending with the PT-30 resin. Cured PT-30/30B (97.5/2.5) THF and PT-30/30B (96.5/3.5) THF samples were prepared for TEM analyses. Cloisite® 30B is uniformly dispersed in PT-30/30B THF system as shown in Figures 2 and 3. At higher magnification Cloisite® 30B is in an intercalated state in the PT-30 resin, larger clay tactoids were observed than when PT-15 was mixed with Cloisite® 30B (see section 3.2) and cured in the same manner.

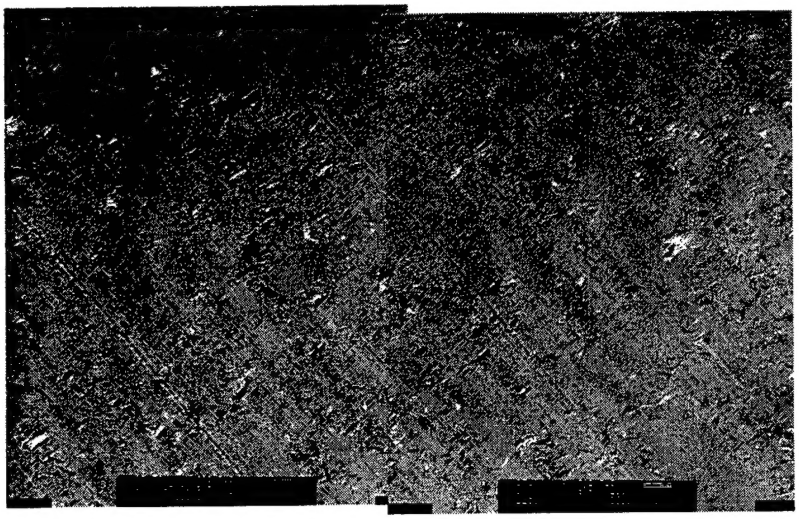

Figure 2 Low magnification TEM micrographs of PT-30/Cloisite® 30B (97.5/2.5) THF showing uniform dispersion of nanoclay Cloisite® 30B in PT-30 cyanate ester where scale bar is 1 μm

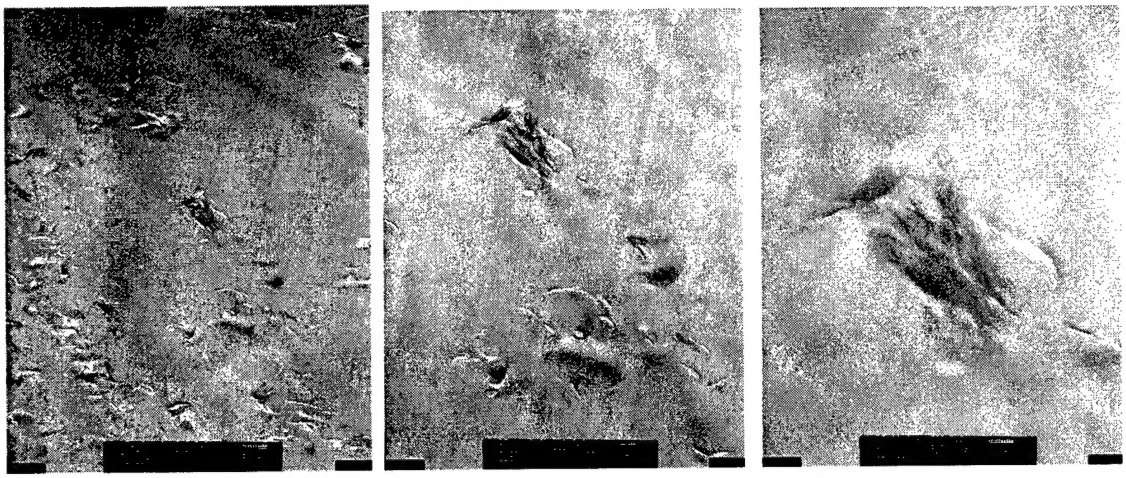

Figure 3 Higher magnification of PT-30/Cloisite® 30B (97.5/2.5) THF showing nanoclay in an intercalated state in the PT-30 cyanate ester resin where scale bars are 500 nm (left), 200 nm (center), and 100 nm (right)

The TEM micrographs of PT-30 (pure), PT-30/SO1458 (95/5) THF-blended, and PT-30/SO1458 (95/5) are shown in Figures 4 through 6. Figure 4 shows the TEM micrograph of a neat PT-30 cyanate ester resin system. Figure 5 shows the TEM micrographs of large SO1458 POSS® particles in the PT-30/SO1458 POSS® (95/5) THF-blended system. The large oval seen in the

center micrograph is not a particle. It is a bubble void in the resin. Using THF to dissolve SO1458 POSS® before blending into the PT-30 was not as beneficial in this case as with PT-15 (see section 3.2). On the other hand, the SO1458 POSS® particles, when directly blended into PT-30 resin shows, very few undissolved POSS® particles in the resin matrix as shown in Figure 6. Some molecular dispersion in the PT-30/SO1458 POSS® (95/5) was achieved as shown in Figure 6. Significant Si is detected in the resin matrix where no phase separation can be detected. SO1458 is the preferred POSS® system for PT-30 resin.

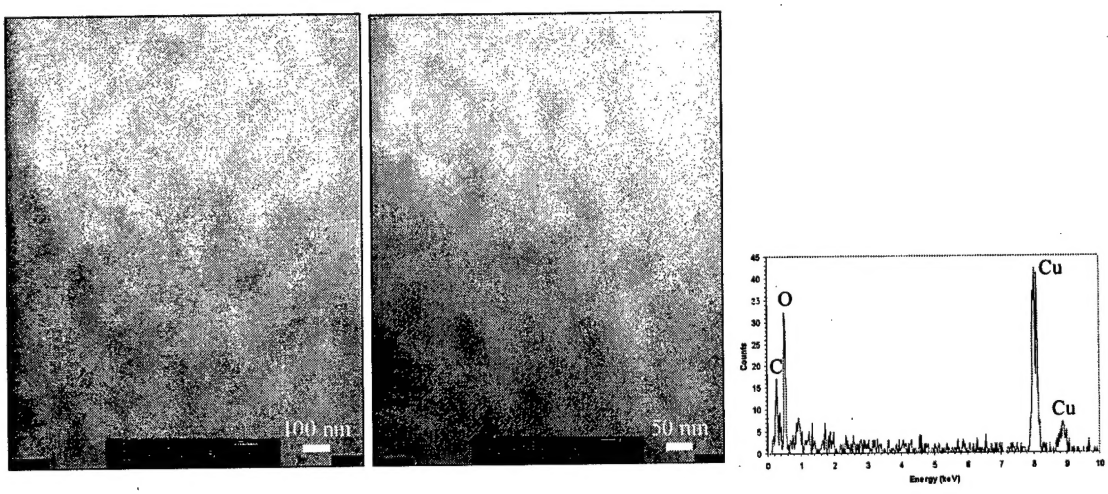

Figure 4 TEM micrographs of a neat PT-30 cyanate ester resin

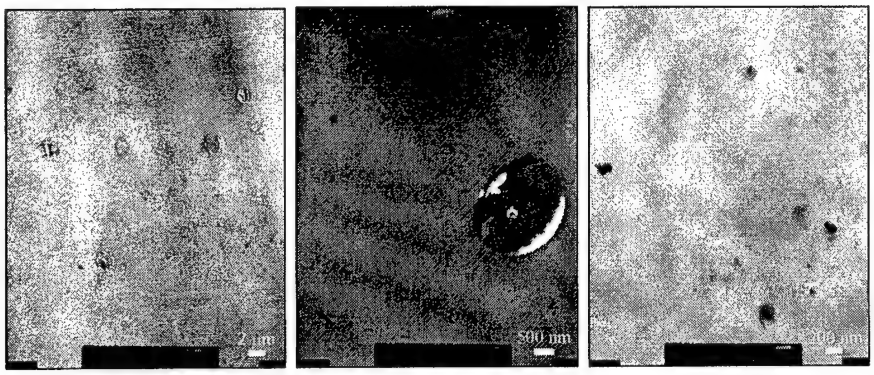

Figure 5 TEM micrographs of PT-30/SO1458 POSS® (95/5) THF showing micron- and nano-sized POSS particles in the PT-30 cyanate ester. In the center micrograph, the large oval object is not a particle. It is a void due to a bubble.

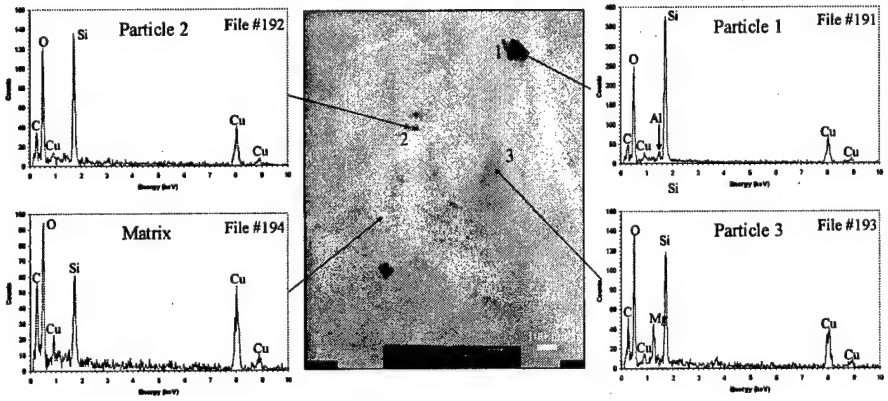

Figure 6 TEM micrographs of PT-30/SO1458 POSS® (95/5) in high magnification showing molecular dispersion of SO1458 POSS® with some POSS® particles in the PT-30 cyanate ester. Significant Si is detected in the resin matrix.

3.2 Processing and Characterization of PT-15/Nanoparticle Systems PT-15 was blended with several clays (Nanomer® I.28E, Nanomer® I.30E, PWG, Cloisite® 10A, and Cloisite® 30B) using different mixing methods, a total of 34 blends were recorded. Resulting samples were either opaque or translucent.

PT-15/30B (97.5/2.5) THF, PT-15/10A (97.5/2.5) THF, and PT-15/I.30E (97.5/2.5) THF blends were prepared using THF as a carrier medium in these samples to facilitate clay dispersion. All three clays show uniform dispersion as shown in Figures 7 through 9. When Cloisite® 30B, Cloisite® 10A, and Nanomer® I.30E were compared in higher magnification TEM micrographs, Cloisite® 30B is dispersed slightly more uniformly than the other two clays as shown in Figure 10. Cloisite® 30B is in a partial exfoliated state in PT-15 as shown in Figure 10. Small tactoids are also present in this nanodispersion. Cloisite® 30B is our preferred clay for the PT-15 resin.

PT-15 was blended with PPSQ in THF and trisilanol phenyl POSS® in different wt% and a total of 13 blends were recorded. Only PT-15/trisilanol phenyl POSS® in (99/1) and (97/3) were completely transparent. TEMs of PT-15 (pure), SO1458 POSS® (trisilanol phenyl POSS®), PT-15/SO1458 (97/3), & PT-15/SO1458 (95/5) blends are shown in Figures 11 through 15. Figure 11 shows the TEM of the neat PT-15 resin. The SO1458 POSS® are micron-sized particles in IPA solvent as shown in Figure 12. Figures 13 and 14 show molecular dispersion of SO1458 POSS® in the PT-15/SO1458 (97/3) system. Where particles are noted, one finds their Si content is higher than in the open resin matrix. Significant Si is detected in the resin matrix in regions where no particles are observed. Clearly, the POSS® is partially dissolved in the matrix and partially nanodispersed. This is a good candidate system for a conversion to CCC. Figure 15 shows similar molecular dispersion of SO1458 POSS® in the PT-15/SO1458 (95/5) system. SO1458 POSS® is the preferred POSS® system for the PT-15 resin.

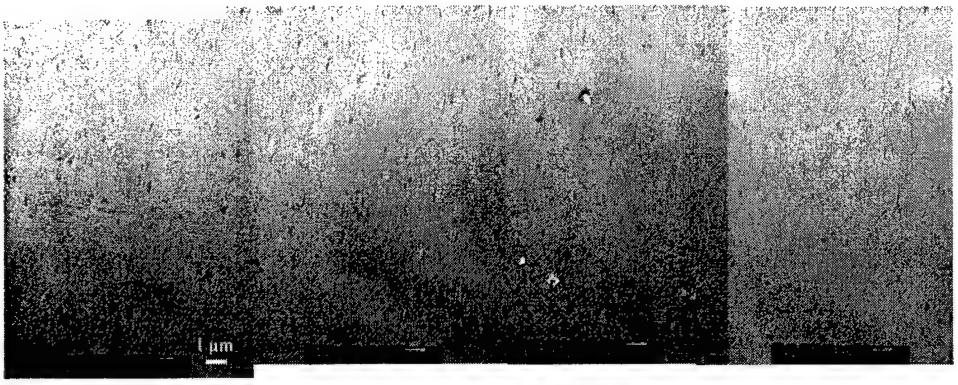

Figure 7 TEM micrographs of PT-15/Cloisite® 30B (97.5/2.5) THF showing uniform dispersion of Cloisite® 30B in the PT-15 cyanate ester where scale bar is 1 µm

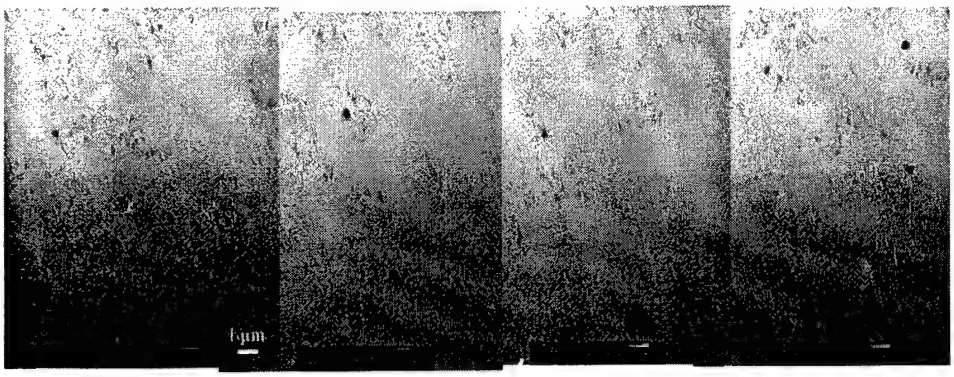

Figure 8 TEM micrographs of PT-15/Cloisite® 10A (97.5/2.5) THF showing uniform dispersion of Cloisite® 10A in PR-15 cyanate ester where scale bar is 1 μm

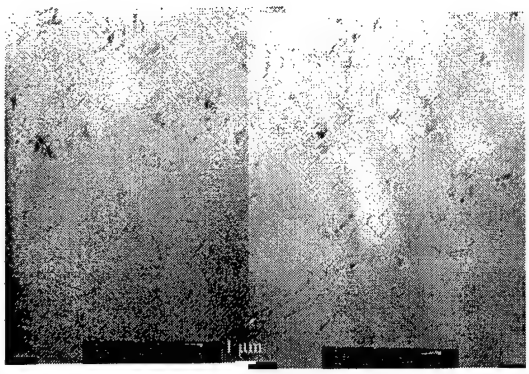

Figure 9 TEM micrographs of PT-15/Nanomer® I.30E (97.5/2.5) THF showing uniform dispersion of Nanomer® I.30E in PT-15 cyanate ester where scale bar is 1 μm

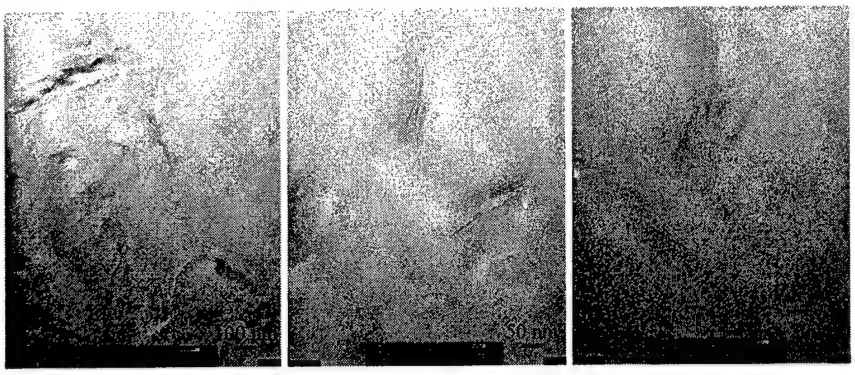

Figure 10 Higher magnification TEM micrographs of PT-15/Cloisite® 30B (97.5/2.5) THF showing Cloisite® 30B clays are exfoliated in PT-15 cyanate ester

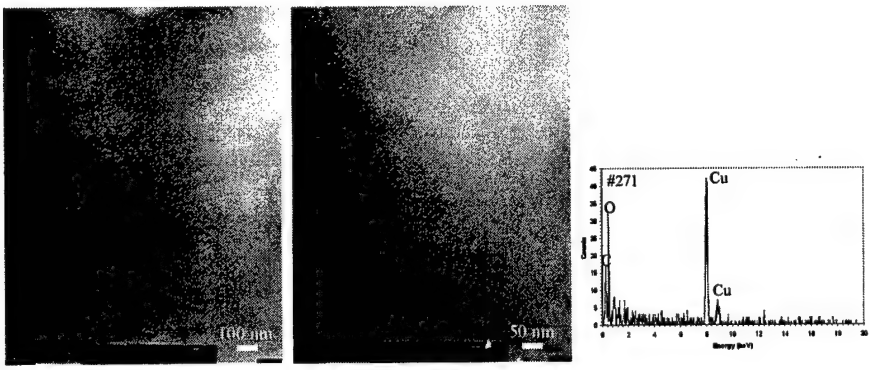

Figure 11 TEM micrographs of a neat PT-15 cyanate ester resin

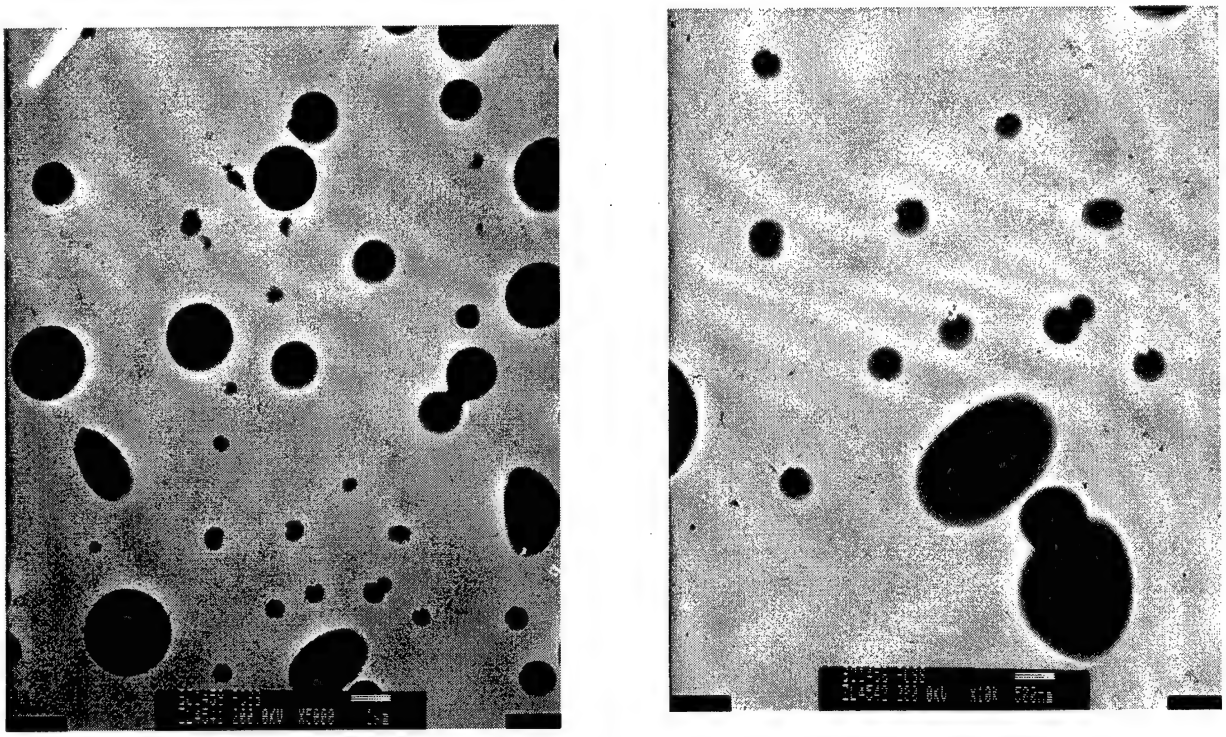

Figure 12 TEM micrographs of micron-sized SO1458 POSS® (trisilanol phenyl POSS®) particles in an IPA solvent where scale bar is 1μm (left) and scale bar is 500 nm (right)

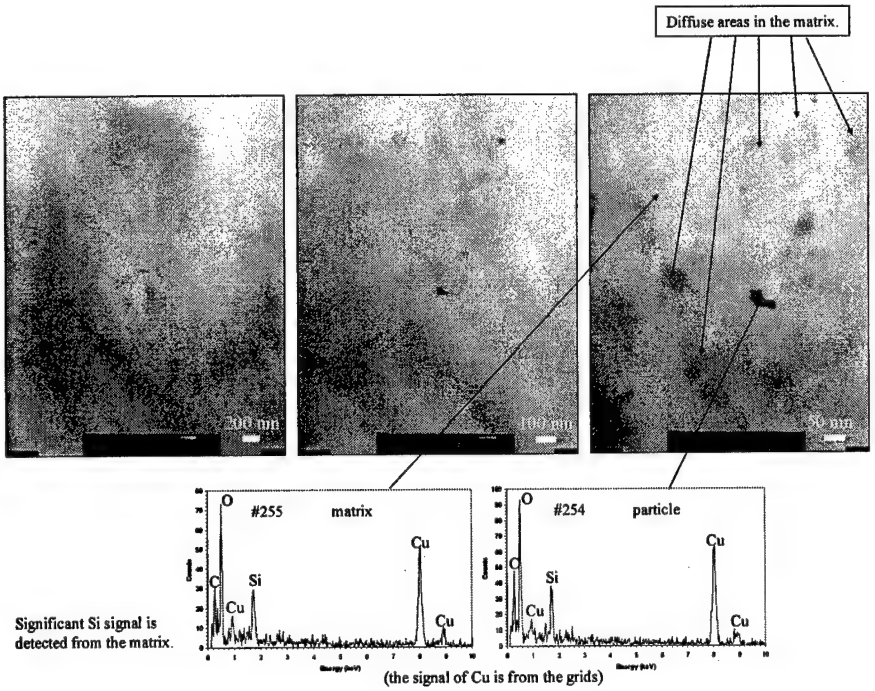

Figure 13 Progressive magnification TEM micrographs of PT-15/SO1458 POSS® (97/3) showing molecular dispersion of SO1458 POSS® in PT-15 cyanate ester. Si from POSS® molecules is dispersed in the resin matrix. The dark particle has the same Si/O/C composition as the resin matrix.

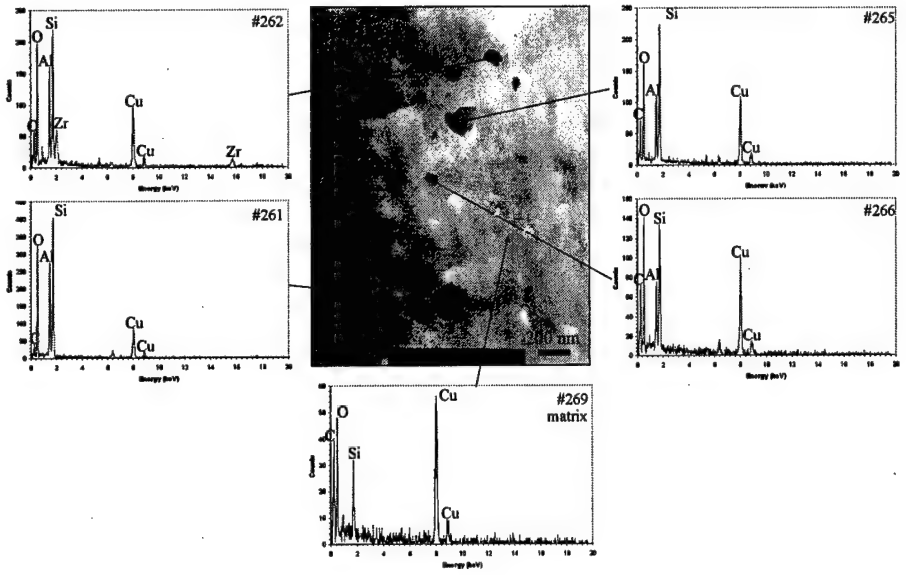

Figure 14 Higher magnification TEM micrographs of PT-15/SO1458 POSS® (97/3) showing molecular dispersion of SO1458 POSS® particles in PT-15 cyanate ester. Si is dispersed in the resin matrix. The particles have more Si content than resin.

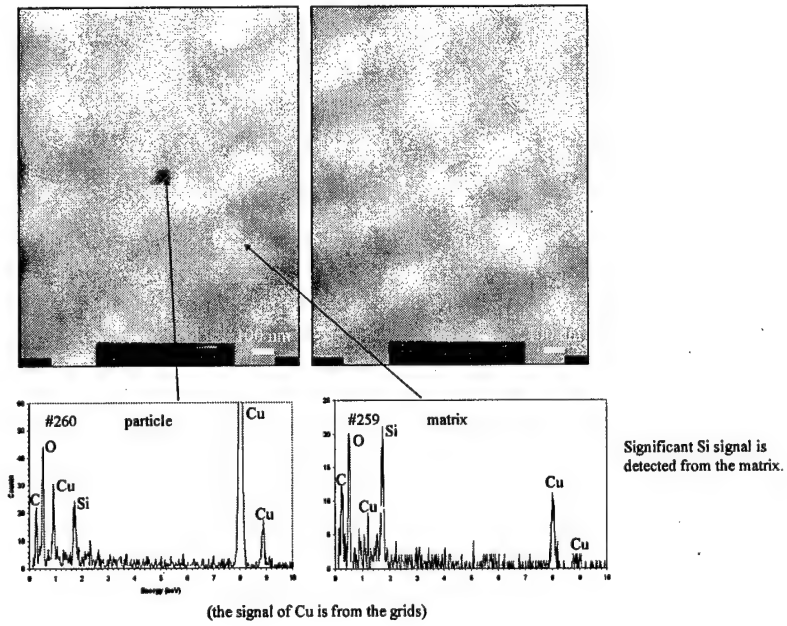

Figure 15 TEM micrographs of PT-15/SO1458 POSS (95/5) in high magnification showing molecular dispersion of SO1458 POSS molecules in PT-15 cyanate ester. Significant Si is detected in the resin matrix.

3.3 Processing and Characterization of 134A/Nanoparticle Systems Phenolic resin 134A in IPA was mixed with a clear solution of dichloromethylsilylethyl isobutyl POSS® in THF. Also, 134A/trisilanol phenyl POSS® in THF in (99/1), (97/3), and (90/10) were studied. 134A/Cloisite® 10A IPA were blended in compositions of (98/2), (95/5), and (90/10). XRD analyses showed that a portion of the clay appeared very similar to that of the pure as-received Cloisite® 10A and another portion had contracted to a smaller d-spacing than that of the original as-received clay. Based on previous studies on SC 1008 phenolic resin [5] we selected Cloisite® 30B as the preferred nanoclay for the 134A phenolic.

Hitco 134A/ dichloromethylsilylethyl isobutyl POSS® in THF in (97/3) and (90/10) were examined using TEM analysis. Micron- and nano-sized POSS particles were observed in the 134A resin matrix indicating this POSS chemical is not compatible with the phenolic. Apparently, the two Si-Cl bonds react with IPA faster than with phenolic resin hydroxyl groups. The resulting POSS® molecule is not highly soluble in the resin. Based on previous studies on the SC 1008 phenolic resin [5] we selected SO1458 POSS® as the preferred POSS® for the 134A phenolic.

3.4 Scaling Up and Processing of CCC Based on TEM analyses six candidates were selected for scale up at Hitco and Extrusion Technology in the following six compositions and wt% range:

- 134A/Cloisite® 30B in (95-99/5-1) wt%
- 134A/SO1458 POSS® in (95-99/5-1) wt%
- PT-15/Cloisite® 30B in (95-99/5-1) wt%
- PT-15/SO1458 POSS® in (95-99/5-1) wt%
- PT-30/Cloisite® 30B in (92.5-97.5/75-2.5) wt%
- PT-30/PR-24-PS in (99.5-99/0.5-1) wt%

Based on the scale up studies, the final compositions of the six candidates to produce prepregs at Hitco were:

- 134A/Cloisite® 30B in (97/3) wt%
- 134A/SO1458 POSS® in (97/3) wt%
- PT-15/Cloisite® 30B in (95/5) wt%
- PT-15/SO1458 POSS® in (95/5) wt%
- PT-30/Cloisite® 30B in (95/5) wt%
- PT-30/PR-24-PS in (99/1) wt%

An overall procedure of processing, fabrication, thermo-oxidative and mechanical properties testing of all the NCCCs and CC139 is outlined in Figure 16.

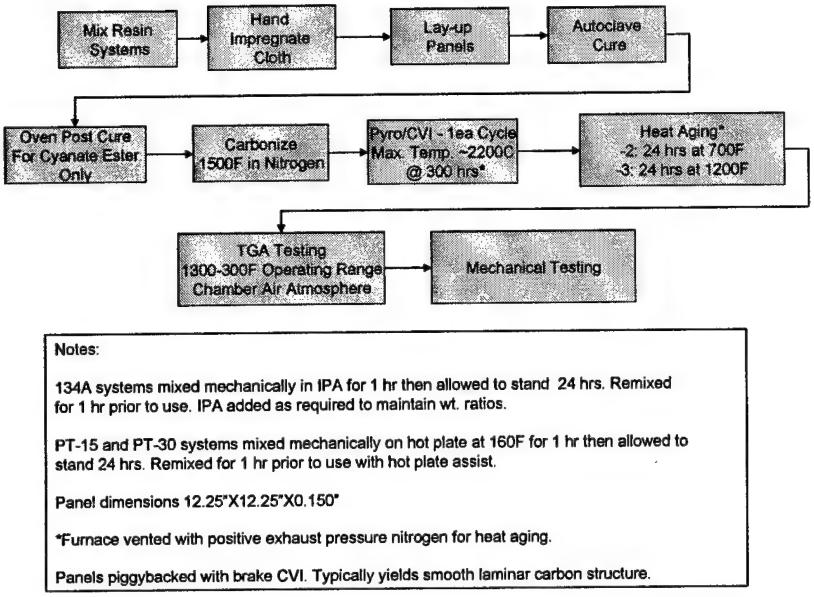

Figure 16 Overall procedures for processing, fabrication, thermo-oxidative, and mechanical testing of NCCCs and CC139

Processing Procedures Hitco uses the same T-300 carbon fiber fabric that is used for CC139 for all six CCC candidates. The fabric is prepregged by hand in Hitco's R&D lab using the pre-determined resin/filler compositions. All panels are consolidated by vacuum bagging and autoclave cured at appropriate temperature cycles. Panels are physically characterized for dimensions and weight. Cured panel is carbonized in inert gas (nitrogen) to 1,500°F, then cooled and characterized for density and porosity. All panels are co-processed in Hitco's proprietary carbon CVI process to achieve a target density of 1.7 g/cc within two cycles. At the completion of the processing, all panels are given a final characterization for density and porosity. One witness panel of each type will be processed, with samples removed for archiving at the cure, carbonized and fully infiltrated stages. A set of four 12- by 12- by 0.15-inch CCC panels are be fabricated for each candidate and CC139, a total of 28 panels are manufactured. Figure 17 shows the nanomodified C/C composite (NCCC) panels.

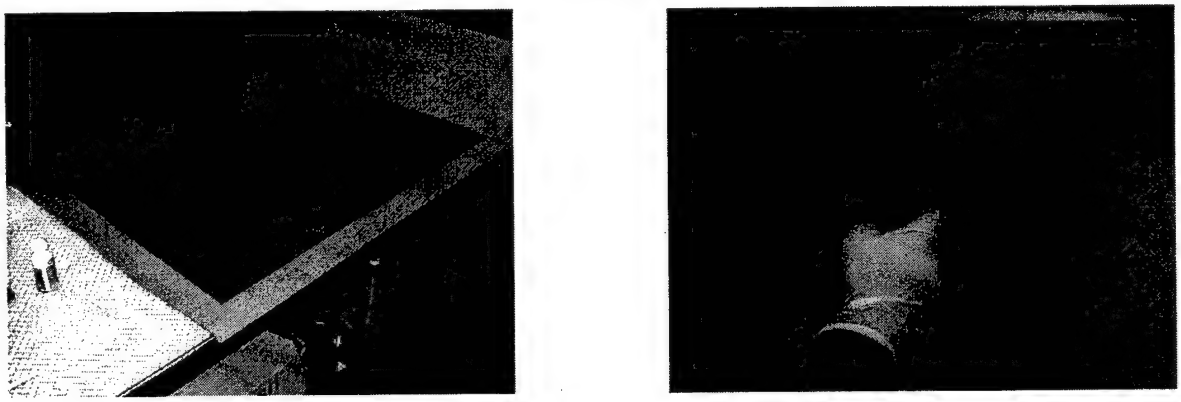

Figure 17 NCCC 12.25- by 12.25- by 0.15-inch panels (left) and close-up NCCC panels (right)

Hitco conducted exposure testing of panels to determine the magnitude of the benefit of each materials variation. Hitco provided QA testing for heat exposure for a number of its current products using several small capacity air muffle furnaces.

The four panels of the seven C/C composites were tested in the following manner:

- One panel was heat aged for 24 hrs at 1,200°F
- One panel was heat aged for 24 hrs at 700°F
- One panel was reserved for room temperature
- One panel was a spare

Samples were removed from the furnace for brief periods for spot measurement of weight loss. At the completion of the 24 hr. exposure, mechanical test coupons were machined for the panels and tested for tensile, compressive, and flexural strengths and modules.

3.5 Thermo-oxidative Studies of CCC Physical properties of NCCC materials such as averaged bulk density, skeletal density, and porosity data were recorded as shown in Table 2. Porosity is a measure of how much pyrocarbon could be added to the CCC. One panel from each candidate was subjected to 24 hrs at 700°F and 1,200°F in nitrogen. Samples were removed from the furnace for brief periods for spot measurement of weight loss. After the 24 hrs exposure, TGA furnaces were used to record weight loss using a set volume of air flow to simulate oxidation on the *RT, 700°F, and 1,200°F specimens designated as -1, -2, and -3, respectively.* Air flow was set at 2 L/min and approximately 10°C/hr ramp rate to 1300°F. All specimens were exposed for 8 hrs. Figures 18 to 23 show typical temperature and weight loss data of the thermo-oxidative studies for selective NCCC specimens that were RT, heat aged 700°F and 1,200°F.

Table 2 Summary of Physical Data of NCCCs

P/N	Bulk Density (g/cc)	Skeletal Density (g/cc)	Porosity (%)	Conditions	Rank
134A/CLO/3-1	1.619	1.816	10.8	-1 RT	
134A/CLO/3-2	1.581	1.831	13.7	-2 700°F	
134A/CLO/3-3	1.567	1.815	13.7	-3 1,200°F	
134A/CLO/3-4	1.585	1.816	12.7	-4 Spare	5
134A/POSS/3-1	1.616	1.814	10.9	-1 RT	
134A/POSS/3-2	1.575	1.804	12.7	-2 700°F	
134A/POSS/3-3	1.611	1.813	11.1	-3 1,200°F	
134A/POSS/3-4	1.603	1.801	11.0	-4 Spare	4
PT15/POSS/5-1	1.651	1.797	8.1	-1 RT	
PT15/POSS/5-2	1.595	1.804	11.6	-2 700°F	
PT15/POSS/5-3	1.626	1.804	9.8	-3 1,200°F	
PT15/POSS/5-4	Lost			-4 Spare	
PT15/CLO/5-1	In	Preparation			
PT15/CLO/5-2	In	Preparation			
PT15/CLO/5-3	In	Preparation			
PT15/CLO/5-4	In	Preparation			
PT30/PR24PS/1-1	1.630	1.773	8.1	-1 RT	
PT30/PR24PS/1-2	1.643	1.775	7.4	-2 700°F	
PT30/PR24PS/1-3	1.684	1.889	10.8	-3 1,200°F	
PT30/PR24PS/1-4	1.667	1.876	11.1	-4 Spare	2
PT30/CLO/5-1	1.653	1.906	13.3	-1 RT	1
PT30/CLO/5-2	1.656	1.913	13.4	-2 700°F	1
PT30/CLO/5-3	1.618	1.917	15.6	-3 1,200°F	1
PT30/CLO/5-4	1.653	1.898	12.9	-4 Spare	1
CC139-1	1.627	1.801	9.7	-1 RT	3
CC139-2	1.638	1.801	9.1	-2 700°F	3
CC139-3	1.630	1.799	9.4	-3 1,200°F	3
CC139-4	1.644	1.801	8.7	-4 Spare	3

* RT, 700°F, and 1,200°F specimens were designated as -1, -2, and -3, respectively.

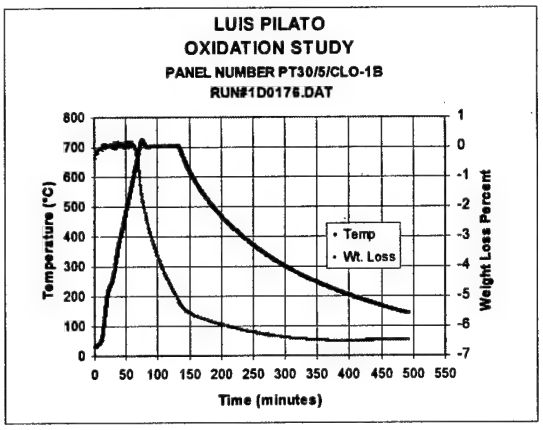

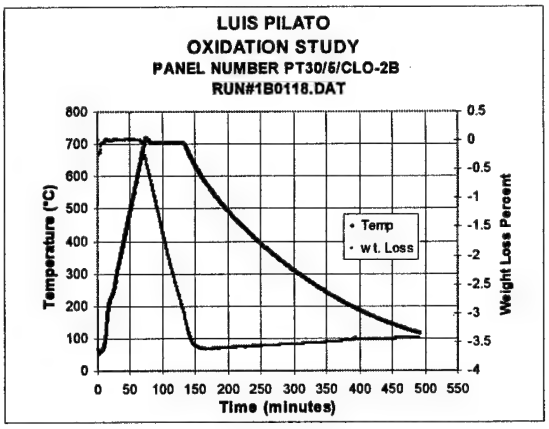

Figure 18 Thermo-oxidative study of PT30/CLO/5-1B RT specimen (left) and PT30/CLO/5-2B 700°F specimen (right) heat aged in air for 8 hrs

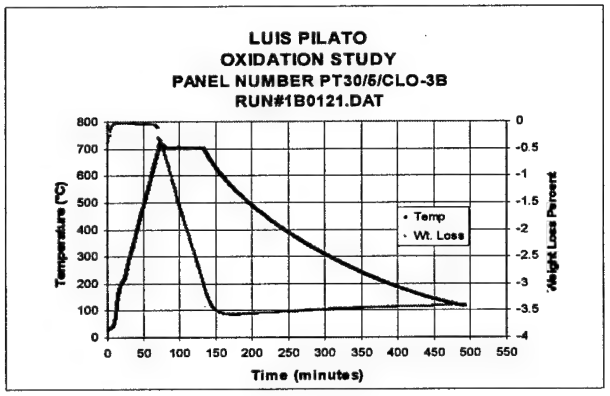

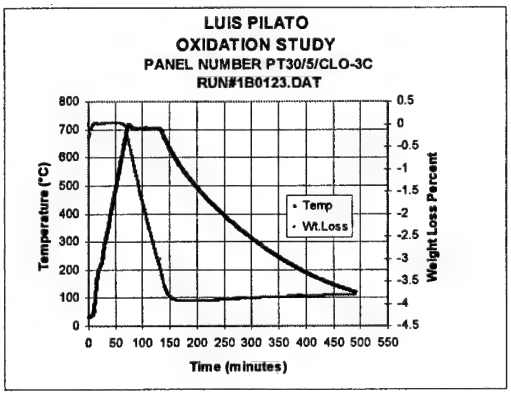

Figure 19 Thermo-oxidative study of PT30/CLO/5-3B 1,200°F specimen (left) and PT30/CLO/5-3C 1,200°F specimen (right) heat aged in air for 8 hrs

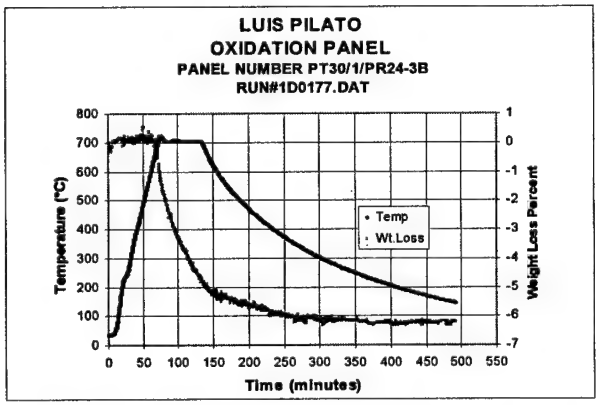

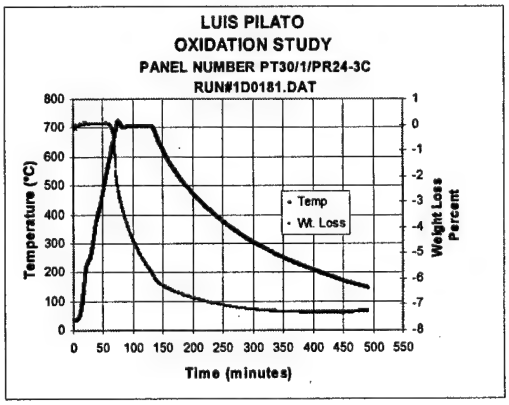

Figure 20 Thermo-oxidative study of PT30/PR24PS/1-3B 1,200°F specimen (left) and PT30/PR24PS/1-3C 1,200°F specimen (right) heat aged in air for 8 hrs

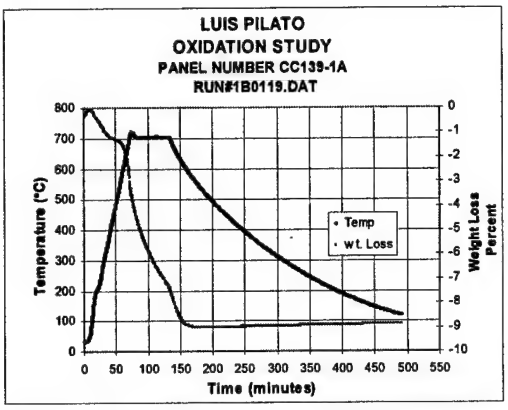

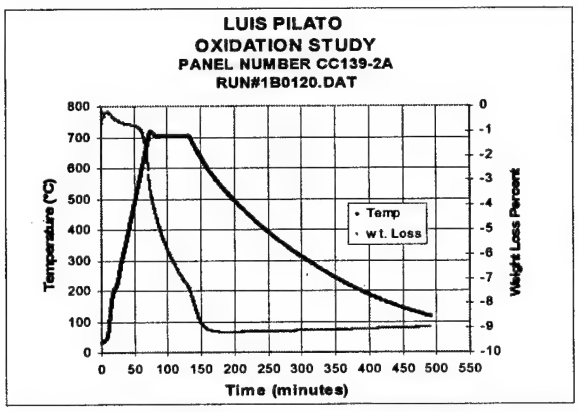

Figure 21 Thermo-oxidative study of CC139-1A RT specimen (left) and CC139-2A 700°F specimen (right) heat aged in air for 8 hrs

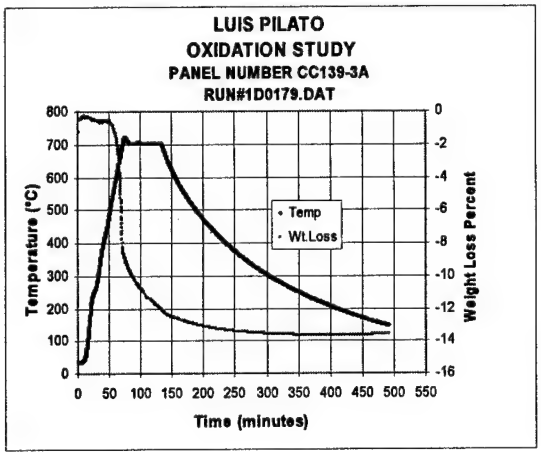

Figure 22 Thermo-oxidative study of CC139-3A 1,200°F specimen heat aged in air for 8 hrs

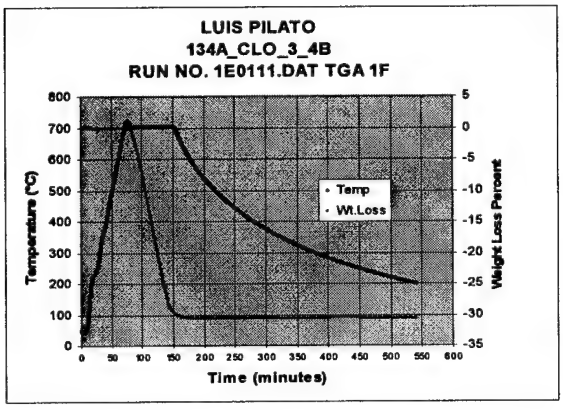

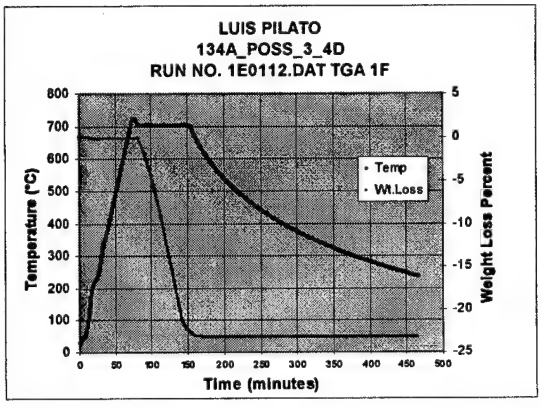

Figure 23 Thermo-oxidative study of 134A/CLO/3-4B 700°F specimen (left) and 134A/POSS/3-4D 1,200°F specimen (right) heat aged in air for 8 hrs

A summary of all the NCCC candidates and CC139 with their weight loss percentage, density, and ranking based on weight loss data is shown in Table 3. An air leakage was detected in our

first set of experiments as a result the 134A/CLO/3-1A, 134A/CLO/3-2A, 134A/CLO/3-3A, 134A/POSS/3-1A, 134A/POSS/3-2A, 134A/POSS/3-3A, PT15/POSS/5/-1B, PT15/POSS/5/-2A, and PT15/POSS/5/-3A specimens were overexposed to unrealistic thermo-oxidative conditions. They are denoted with an * in Table 3. The 134A/CLO/3-4B and 134A/POSS/3-4D specimens were retested for the 1,200°F condition using the fourth spared panels of the 134A/CLO/3 and 134A/POSS/5 candidates marked as "-4" as shown in Figure 23. The PT15/POSS/5-4 spared specimen was lost, and as a result the PT15/POSS/5 candidate will not be retested for the 1,200°F condition for this project. The fabrication of the four test panels of the PT15/CLO/5 candidate was completed and the thermo-oxidative and mechanical properties testing will be completed next month and the data will be reported later elsewhere [7]. Regrettably the behavior of molecularly dispersing POSS® into PT-15 (Table 3, entries 9 to 12) could not be assessed for improved thermo-oxidative stability due to specimens overexposed or lost.

Table 3 Summary of Thermo-oxidative Data and Ranking

P/N	Initial wt (g)	TGA recorded wt. (g)	Weight Loss (%)	Sample Density (g/cc)	Rank
134A/CLO/3-1A*	2.053	1.728	-15.8	1.619	
134A/CLO/3-2A*	2.145	1.772	-17.4	1.581	
134A/CLO/3-3A*	2.056	1.152	-44.0	1.567	
134A/CLO/3-4B	2.036	1.414	-30.5	1.585	5
134A/POSS/3-1A*	1.958	1.441	-26.4	1.616	
134A/POSS/3-2A*	1.989	1.216	-38.9	1.575	
134A/POSS/3-3A*	1.933	1.666	-13.8	1.611	
134A/POSS/3-4D	2.055	1.573	-23.2	1.603	4
PT15/POSS/5-1B*	2.469	2.178	-11.8	1.650	
PT15/POSS/5-2A*	2.462	2.146	-12.9	1.595	
PT15/POSS/5-3A*	2.577	1.782	-30.8	1.651	
PT15/POSS/5-4	Lost				
PT15/CLO/5-1	In	Preparation			
PT15/CLO/5-2	In	Preparation			
PT15/CLO/5-3	In	Preparation			
PT30/PR24PS/1-1A*	2.586	1.244	-51.9	1.630	
PT30/PR24PS/1-2A*	2.574	1.406	-45.4	1.643	
PT30/PR24PS/1-3B,C	2.573	2.399	-6.8	1.684	2
PT30/CLO/5-1B,C	2.522	2.358	-5.2	1.653	1
PT30/CLO/5-2B,C	2.383	2.261	-5.1	1.656	1
PT30/CLO/5-3B,C	2.363	2.265	-3.7	1.618	1
CC139-1A	2.673	2.436	-8.9	1.627	3
CC139-2A	2.506	2.881	-9.0	1.638	3
CC139-3A	2.536	2.191	-13.6	1.630	3

* An air leakage was detected in these experiments. RT, 700°F, and 1,200°F specimens were designated as -1, -2, and -3, respectively.

Based on the thermo-oxidative analyses, the PT30/CLO/5 candidate is the most thermo-oxidative resistant, weight losses were 5.2%, 5.1%, and 3.7% at room temperature (RT), 700°F, and

1,200°F conditions, respectively (see Figures 18 and 19). The PT30/PR24PS/1 NCCC has a low 6.8 % weight loss is the second best thermo-oxidative resistant NCCC candidate (see Figure 20). The standard CC139 is the third best material with a weight loss of 8.9%, 9.0%, and 13.6% for RT, 700°F, and 1,200°F, respectively (see Figures 21 and 22). While the 134A/CLO/3-4B and 134A/POSS/3 had high weight loss of 30.5% and 23.3%, respectively (see Figures 23).

Weight losses of different NCCCs were compared as shown in Figure 24. It is evident that the cyanate ester resin-based PT30/PR24PS/1 and PT30/CLO/5 specimens have better thermo-oxidative resistance than the phenolic resin-based CC139 standard CCCs. The phenolic resin-based 134A/CLO/3 and 134A/POSS/3 specimens have worse thermo-oxidative resistant characteristics than the CC139 standard. From our TEM analyses we concluded that the nanoparticles were dispersed very well in the PT30 and PT15 cyanate resin systems and poorly in the 134A phenolic resin system. Figure 25 shows a comparison of the density of the different NCCCs. It is also evident that PT30/PR24PS/1-3B,C has the highest density (1.684 g/cc), followed by PT30/CLO/5-2B,C (1.656 g/cc) and PT30/CLO/5-1B,C (1.653 g/cc), then the CC139 specimens (1.627 to 1.638 g/cc), while the densities of 134A/POSS/3-4D and 134A/CLO/3-4B were 1.603 g/cc and 1.585 g/cc, respectively. Figure 26 shows a comparison of densities versus weight loss of the different NCCCs. A trend of higher density NCCCs exhibiting lower weight loss while lower density NCCCs show higher weight loss is proposed. Lower weight loss for NCCC from cyanate ester resin systems is expected due to little or no volatiles from cured cyanate esters as well as proposed improved thermo-oxidative stability attributable to the presence of a nanophase in the NCCC cyanate ester materials.

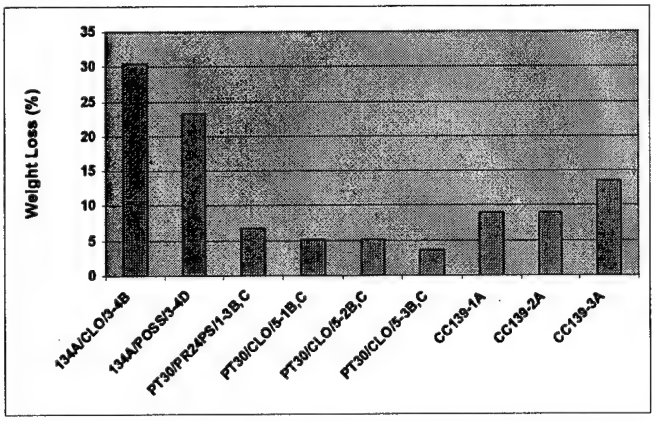

Figure 24 Comparison of weight loss with different NCCCs

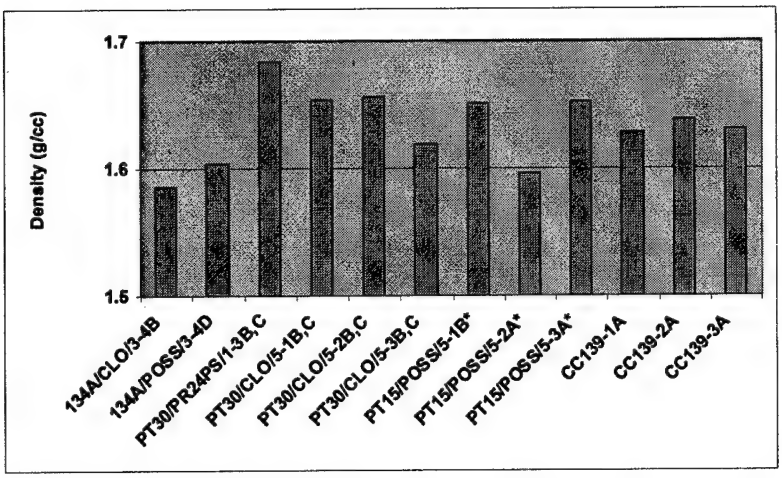

Figure 25 Comparison of density of different NCCCs

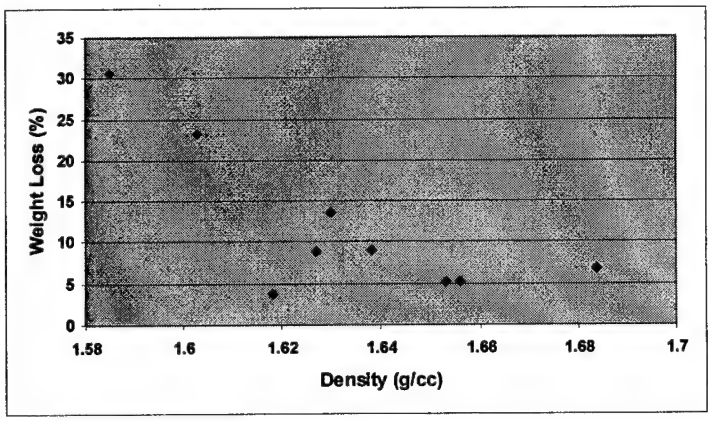

Figure 26 Comparison of density and weight loss of different NCCCs

3.6 Mechanical Properties of CCC All four NCCCs (134A/CLO/3, 134A/POSS/3, PT30/CLO/5, PT30/PR24PS/1) and CC139 panels were visually inspected and tap tested to identify blisters (delamination defects) and data recorded. Specimen was extracted from detect free (as much as possible) areas. All interlaminar test specimens were visually defect free areas while some tensile specimens had to be cut from the blistered areas (Table 4). Figure 27 shows a schematic of our mechanical test plan and a summary of the mechanical properties of the NCCC samples that were measured. Tension and interlaminar shear (4-point short beam shear) tests were conducted per ASTM using at least 3 specimens. All interlaminar shear strength (ILSS) tests were successful and the failure modes were delaminations near the mid-plane as expected. The average ILSS of CC139-4, 134A/CLO/3-4, 134A/POSS/3-4, PT30/CLO/5-4, and PT30/PR24PS/1-4 panels at room temperature were 2,834, 1,694, 1,923, 2,086, and 2,236 psi, respectively. The heat-treated (1,200°F) CC139-3, PT30/CLO/5-3, PT30/PR24PS/1-3 panels lost 3, 9, and 13% of the ILSS, respectively (Table 5). The room temperature ILSS of CC139 agreed well with CCMR/NCA&TSU manufactured PT30/T300 based C/C composite panels about 2.5 ksi [1, 2].

Mechanical Test Plan
Nano-Composite Polymer CCC Panels

- **Tension Test:** **ASTM D 3039-00** [1]

[1] Width – 3 Unit Cells (Cell = 0.34-in)

- **4-Pt Short Beam Shear Test:** **ASTM D 7904** [2]

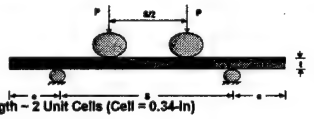

[2] Length – 2 Unit Cells (Cell = 0.34-in)

- Minimum of (3) Specimens Per Panel
- Minimum of (3) Material Systems
- RT & (1) Heat Treated Panel of Each Material System Tested

Material Systems Selected For Testing:

134A/CLO/3 RT & 1200F
PT15/POSS/5 RT & 1200F
PT30/PR24PS/1 RT & 700F

Test	Specimen	Properties		
		Modulus	Strength	Poisson's Ratio
Tension [1]	1	X	X	X
	2	X	X	X
	3	X	X	X
	Avg.	X	X	X
ILSS [2]	1		X	
	2		X	
	3		X	
	Avg.		X	
[1] Modified For Unit Cell Size				
[2] Interlaminar Strength				

Figure 27 Schematic show the mechanical test plan and the NCCC materials that were tested

Tensile modulus, strength and Poisson's ratios were measured for all five material systems. Tensile testing of some of the panels tab slippage problems were due to poor interfacial bonding between the base material and the CVI deposited carbon. It was resolved by abrading the tabbing surfaces. The room temperature Elastic modulus of CC139-4, 134A/CLO/3-4, 134A/POSS/3-4, PT30/CLO/5-4, and PT30/PR24PS/1-4 were 13.0, 17.0, 16.8, 13.8, and 14.3 msi, respectively as shown in Tables 5 through 7. An increase in elastic modulus for NCCCs as compared to baseline CC139 is attributed to nanophase formation. The heat-treated panels lost 3, 2, and –6% of the modulus, respectively as shown in Tables 6 through 10.

Table 4 Quality Analysis of as Received Panels in Batch No. 2

Panel Number	Resin	Filler	wt. %	Heat Treat[1] (F)	Tap Test (manual)	Blistered[2]	Panel Warp	Panel Area (in)	Panel Thickness[3] (in)	TGA weight loss (%)
PT30/CLO/5-3	PT30	Closite	5	1200	Yes	Yes	Yes	12 X 12	0.153	3.7
PT30/CLO/5-4	PT30	Closite	5	none	Yes	Yes	Yes	12 X 12	0.165	-
CCC139-3	134A	Carbon Black	?	1200	Yes		Yes	12 X 12	0.177	13.6
CCC139-4	134A	Carbon Black	?	none	Yes		Yes	12 X 12	0.177	-
PT30/PR24PS/1-3	PT30	PR24PS	1	1200	Yes	Yes	Yes	12 X 12	0.165	6.8
PT30/PR24PS/1-4	PT30	PR24PS	1	none	Yes	Yes	Yes	12 X 12	0.170	-
134A/POSS/3-4	134A	POSS		none	Yes	No		12 X 12	0.136	-
134A/CLO/3-4B	134A			none	Yes	No		12 X 12	0.138	-

Note(s):

1) Heat Treatment Process is 24-hrs in N_2 followed by 4-hrs in air.
2) Average Blister diameter = 3.5-in.
3) Panels have taper in thickness from center to edges (center = greatest thickness).
4) All PT30-based material systems had weak CVD coating surface interface resulting in tab slippage. Additional specimens will be tabbed and tested.

The PT30/PR24PS/1-3, -4 specimens had the highest UTS. It exhibited the largest maximum failure load (both RT and 1,200°F heat-aged specimens) and gradually fell off to 75% load until complete fracture. This indicated that the CNF would enhance ductility while increasing the ultimate strength of the NCCC. The nanoclay specimens were significantly weaker and also had excessive blisters. Nanoclay may hurt the CCC if proper heating cycling is not used in the pyrolysis of the as-cured panels. All of the PT30 materials fracture inside of the tab area with greatest tendency to fail at the actuator end. All PT30 materials had micro-cracking as well as some blistering, particularly the PT30/CLO/5-3 and -4 specimens which had blister near the mid-plane and surface plies. The strength of CC139 panels without and with heat treatment were 46.5 and 47.8 ksi, the difference is less than the one STD of the data. Detailed results in the form of tables (Tables 4 through 10), pictures, and plots (Figures 28 through 43) will follow. Table 11 compares the UTS, elastic modulus, Poisson's ratio and ILSS for the six materials at RT and heat aged conditions. All nanomodified samples, except PT30/CLO/5-4, exhibited higher room temperature strength and modulus compared to control CC139-4.

Panel Inspection Analysis (Visual and Tap Test) No Blisters or delaminations were found in 134A-based panels. PT30-based panels had delaminations, blisters, and micro cracks within the layer. PT30/CLO/5 panels had greatest amount of defects. Blister diameters in PT30-based panels ranged from 2- to 5-inches in diameter. Blisters were located under the surface plies and near the mid-plane of the panel. All panels showed lack of or uneven densification. Macro/micro cracks/voids were apparent from 10X & 20X microscopy study. This is predominant in PT30-based panels. It was concluded that the blisters/delaminations were the result of improper heating cycle of as cured composite part.

Table 5 Interlaminar Shear Strength Results from 4-point Short Beam Shear Tests
Displacement rate: 0.05 in/min

Panel No.	Specimen No.	Width b (in)	Thickness t (in)	Lower Span (5t)	Upper Span (2.5t)	Ultimate Load (lbs)	Interlaminar Shear Strength ILSS (psi)
PT30/CLO/5-3	1	0.699	0.158	0.790	0.395	288.0	1,956
	2	0.700	0.158	0.790	0.395	283.3	1,921
	3	0.701	0.158	0.790	0.395	286.1	1,937
					Average:		**1,938**
					STD:		**17**
PT30/CLO/5-4	1	0.704	0.165	0.825	0.413	332.7	2,148
	2	0.704	0.165	0.825	0.413	324.1	2,093
	3	0.704	0.165	0.825	0.413	312.6	2,018
					Average:		**2,086**
					STD:		**65**
CCC139-3	1	0.706	0.177	0.885	0.443	464.0	2,785
	2	0.706	0.177	0.885	0.443	459.9	2,760
	3	0.706	0.177	0.885	0.443	453.2	2,720
					Average:		**2,755**
					STD:		**33**
CCC139-4	1	0.705	0.177	0.885	0.443	463.3	2,785
	2	0.705	0.177	0.885	0.443	476.6	2,865
	3	0.705	0.177	0.885	0.443	474.8	2,854
					Average:		**2,834**
					STD:		**43**
PT30/PR24PS/1-3	1	0.705	0.170	0.825	0.413	298.6	1,869
	2	0.705	0.170	0.825	0.413	316.3	1,979
	3	0.705	0.170	0.825	0.413	316.7	1,982
					Average:		**1,943**
					STD:		**65**
PT30/PR24PS/1-4	1	0.703	0.165	0.850	0.425	347.7	2,248
	2	0.703	0.165	0.850	0.425	352.8	2,281
	3	0.703	0.165	0.850	0.425	337.1	2,180
					Average:		**2,236**
					STD:		**52**
134A/POSS/3-4	1	0.705	0.136	0.680	0.340	239.1	1,870
	2	0.705	0.136	0.680	0.340	245.8	1,923
	3	0.705	0.136	0.680	0.340	252.7	1,977
					Average:		**1,923**
					STD:		**53**
134A/CLO/3-4	1	0.708	0.138	0.690	0.345	223.4	1,715

Specimen Layout Strategy Tensile specimens were selected from areas of each panel where no or least amount of delamination was visually detected. Tensile specimen length in the delaminated panels was increased to 12-inches to prevent splitting open the laminate at the grip-ends of the coupons. ILSS specimens were selected from areas of each panel where no delamination was visually detected and thickness was uniform.

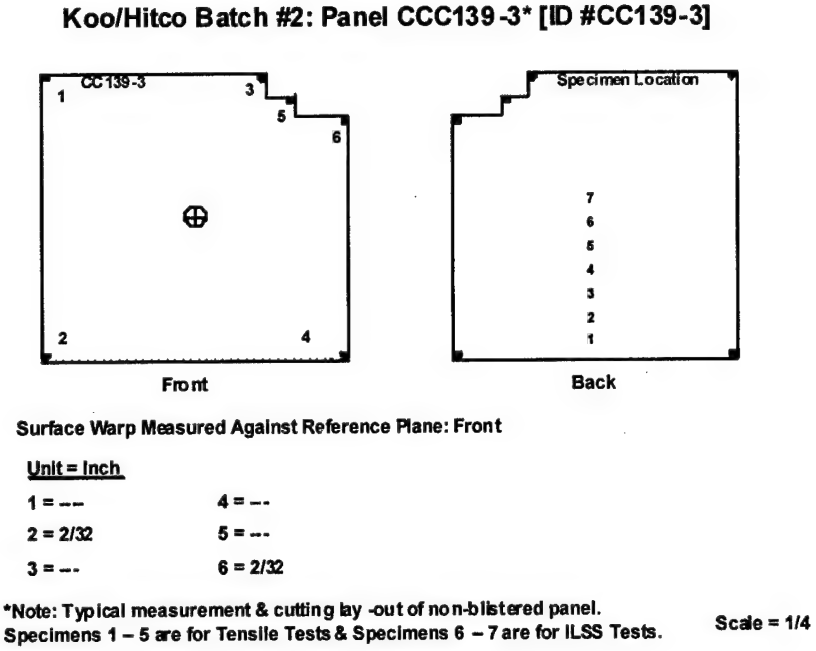

Figure 28 Specimen layout on a non-blistered panel

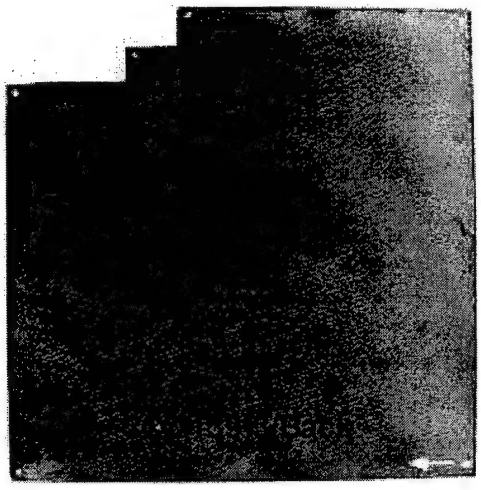

CCC 139-3/Front

Figure 29 Front and back surfaces of a non-blistered panel

Table 6 Tension Test Results for CCC139 Panels
Displacement rate: 0.02 in/min

Panel No.	Specimen No.	Width (in.)	Thickness (in.)	Ultimate Load (lbs)	Ultimate Tensile Strength (psi)	Modulus (Msi)	Poisson's Ratio
CCC139-3	1	1.103	0.169	8,488	45,536	no data	
	2	1.103	0.175	9,271	48,035	13.39	
	3	1.103	0.179	9,853	49,914	12.22	0.111
				Average:	**47,828**	**12.81**	
				STD:	**2,207**	**0.82**	
CCC139-4	1	1.101	0.171	8,411	44,668	14.00	
	2	1.103	0.175	8,871	45,964	12.67	
	3	1.102	0.177	9,513	48,758	12.35	0.074
				Average:	**46,463**	**13.01**	
				STD:	**2,101**	**0.87**	

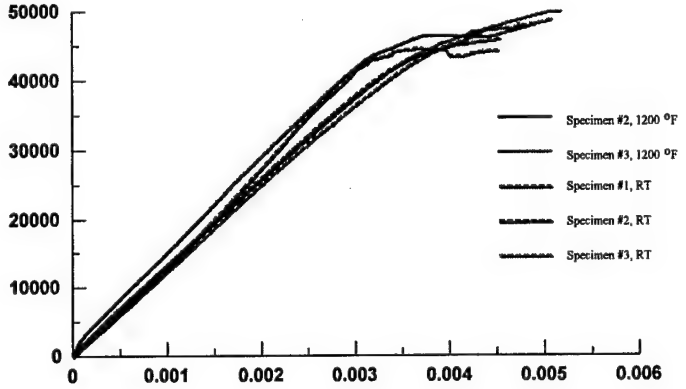

Figure 30 CC139-3 composite stress-strain response

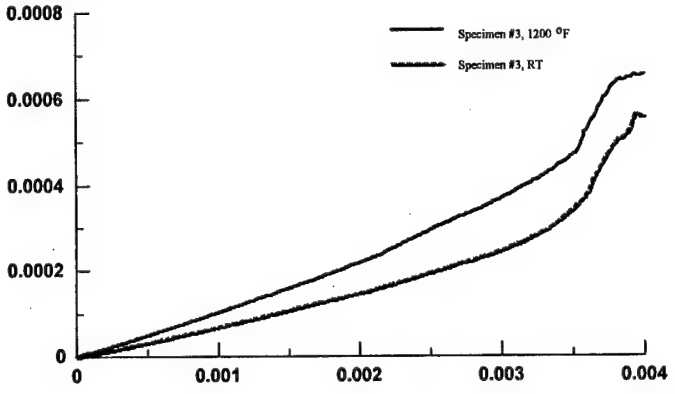

Figure 31 CC139-3 composite axial and transverse strains response

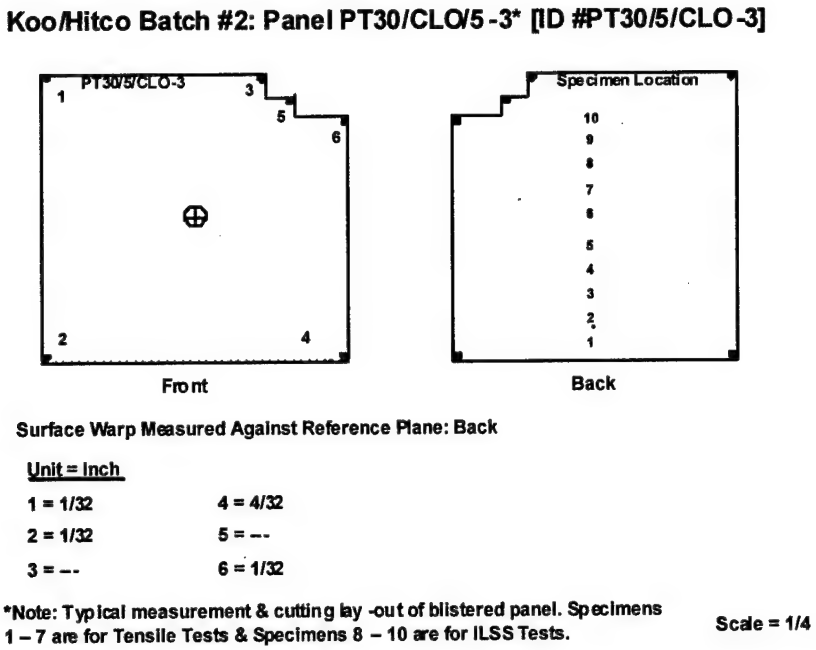

Figure 32 Specimen layout on a blistered panel

PT30/CLO/5-3/Front

Figure 33 Front and back surfaces of a panel with blisters

Table 7 Tension test results for PT30/CLO/5 panels
Displacement rate: 0.02 in/min

Panel No.	Specimen No.	Width (in.)	Thickness (in.)	Ultimate Load (lbs)	Ultimate Tensile Strength (psi)	Modulus (Msi)	Poisson's Ratio
PT30/CLO/5-3	1	1.101	0.163			13.70	0.028
	2	1.102	0.165			15.32	
	3	1.102	0.162			14.93	
	4	1.103	0.167	5,912	32,095		
	5	1.103	0.173	6,652	34,860		
				Average:	**33,478**	**14.65**	
				STD:	N/A	**0.85**	
PT30/CLO/5-4	1	1.101	0.169			14.45	0.036
	5	1.100	0.174			13.98	
	6	1.102	0.174			12.87	
	4	1.102	0.170	8,152	43,514		
	7	1.103	0.171	8,170	43,316		
				Average:	**43,415**	**13.76**	
				STD:	N/A	**0.81**	

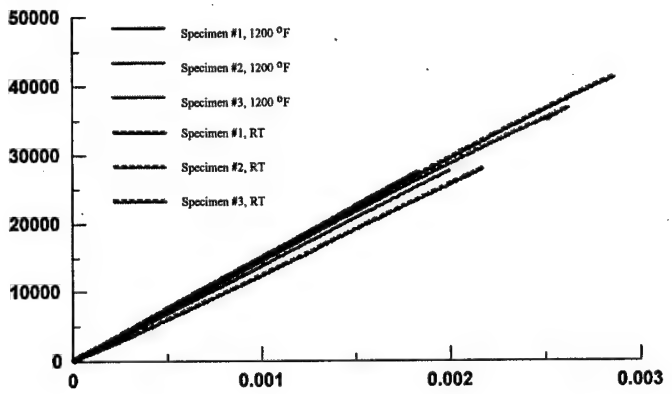

Figure 34 PT30/CLO/5 composite stress-strain response

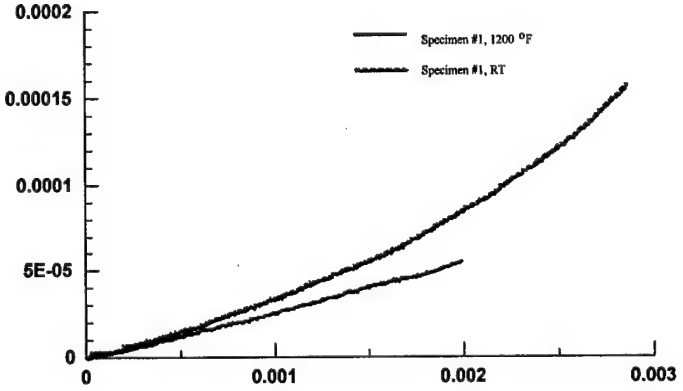

Figure 35 PT30/CLO/5 composite axial and transverse strains response

Table 8 Tension test results for PT30/PR24PS/1 panels
Displacement rate: 0.02 in/min

Panel No.	Specimen No.	Width (in.)	Thickness (in.)	Ultimate Load (lbs)	Ultimate Tensile Strength (psi)	Modulus (Msi)	Poisson's Ratio
PT30/PR24PS/1-3	1	1.102	0.176			14.80	0.033
	2	1.100	0.178			13.62	
	3	1.100	0.179			13.25	
	4	1.101	0.179	11,705	59,392		
	5	1.103	0.173	11,722	61,430		
				Average:	**60,411**	**13.89**	
				STD:		**0.80**	
PT30/PR24PS/1-4	1	1.102	0.165			14.79	0.025
	2	1.102	0.167			14.40	
	3	1.102	0.171			13.75	
	4*	1.102	0.172	10,782	56,884		
	6*	1.103	0.172	11,687	61,603		
				Average:	**59,243**	**14.32**	
				STD:		**0.53**	

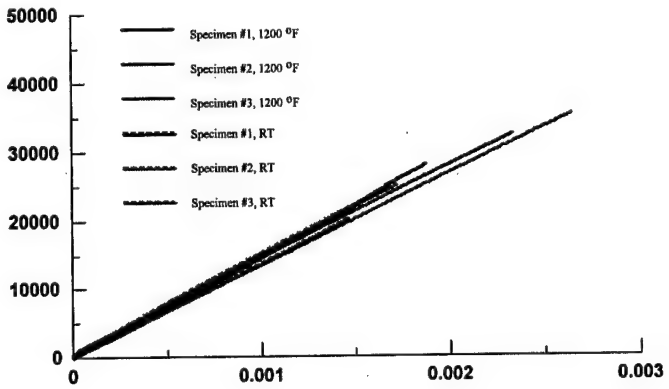

Figure 36 PT30/PR24PS/1 composite stress-strain response

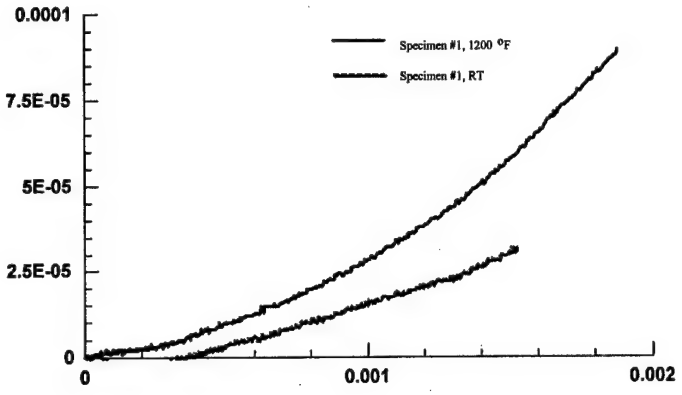

Figure 37 PT30/PR24PS/1 composite axial and transverse strains response

Table 9 Tension Test Results for 134A/POSS/3-4 Pane
Displacement rate: 0.02 in/min

Panel No.	Specimen No.	Width (in.)	Thickness (in.)	Ultimate Load (lbs)	Ultimate Tensile Strength (psi)	Modulus (Msi)	Poisson's Ratio	Transition Strain (in/in)
134A/POSS/3-4	1	1.102	0.136	7,245	48,332	16.30	0.0208	0.0018
	2	1.102	0.138	7,915	52,038	16.64	0.0190	0.0020
	3	1.103	0.137	8,067	53,388	17.43	0.0190	0.0020
				Average:	**51,253**	**16.79**	**0.0196**	**0.0019**
				STD:	**2,618**	**0.58**	**0.0010**	**0.0001**

Note: The modulus and Poisson's ratio were determined in the region where axial strain less than the transitional strain.

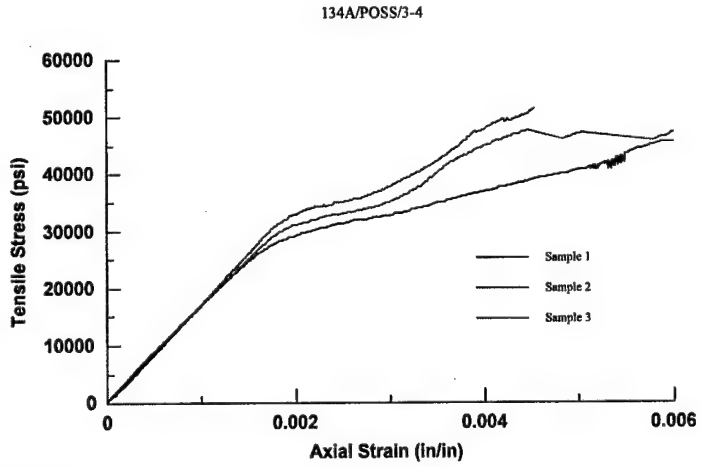

Figure 38 134A/POSS/3-4 composite stress-strain response

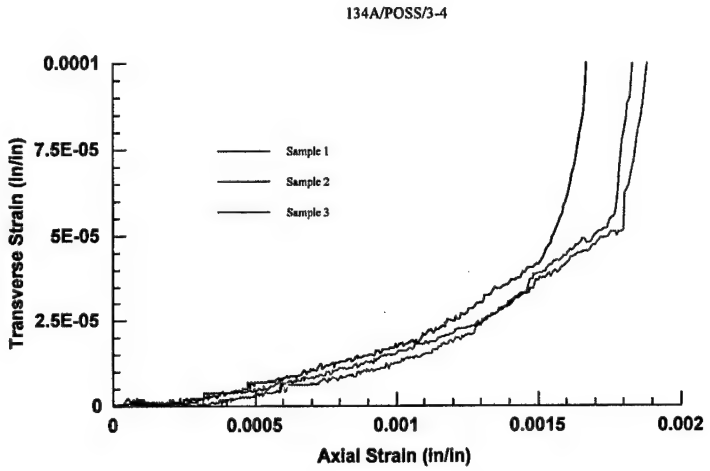

Figure 39 134A/POSS/3-4 composite axial and transverse strains response

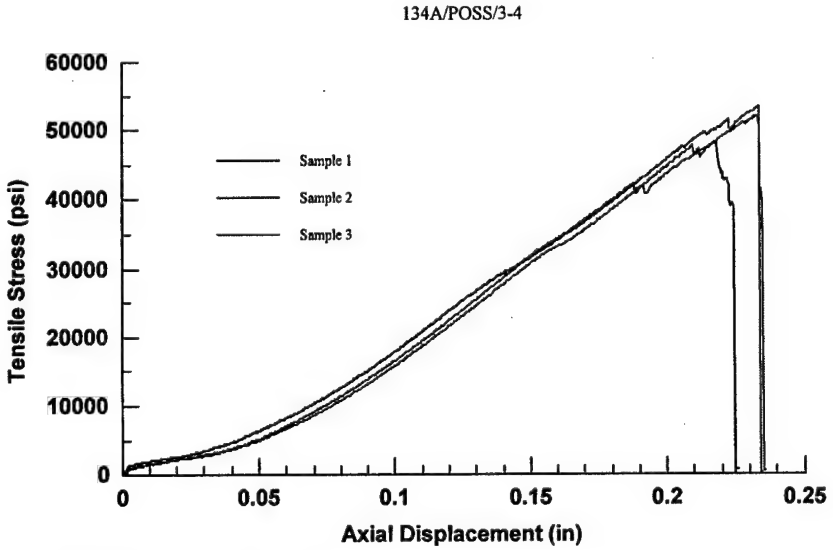

Figure 40 134A/POSS/3-4 composite axial stress-displacement response

Table 10 Tension Test Results for 134A/CLO/3-4 Panel
Displacement rate: 0.02 in/min

Panel No.	Specimen No.	Width (in.)	Thickness (in.)	Ultimate Load (lbs)	Ultimate Tensile Strength (psi)	Modulus (Msi)	Poisson's Ratio	Transition Strain (in/in)
134A/CLO/3-4	1	1.104	0.136	7,827	52,145	17.08	0.0260	0.0019
	2	1.103	0.136	8,067	53,780	17.27	0.0286	0.0018
	3	1.104	0.136	8,057	53,678	16.54	0.0220	0.0018
				Average:	**53,201**	**16.96**	**0.0255**	**0.0018**
				STD:	**916**	**0.38**	**0.0033**	**0.0001**

Note: The modulus and Poisson's ratio were determined in the region where axial strain < transitional strain

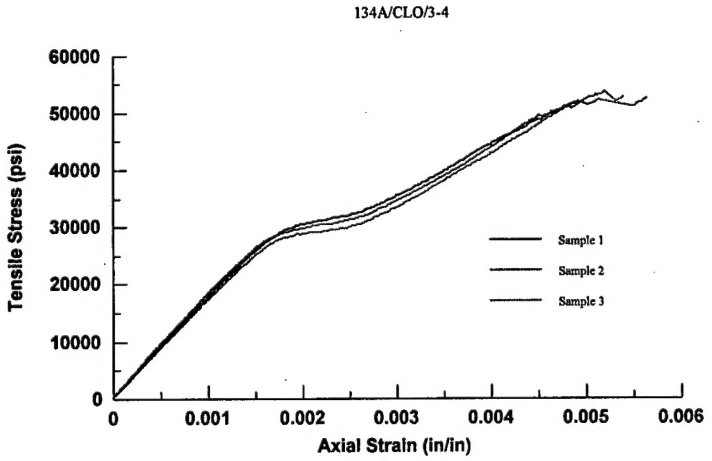

Figure 41 134A/CLO/3-4 composite axial stress-strains response

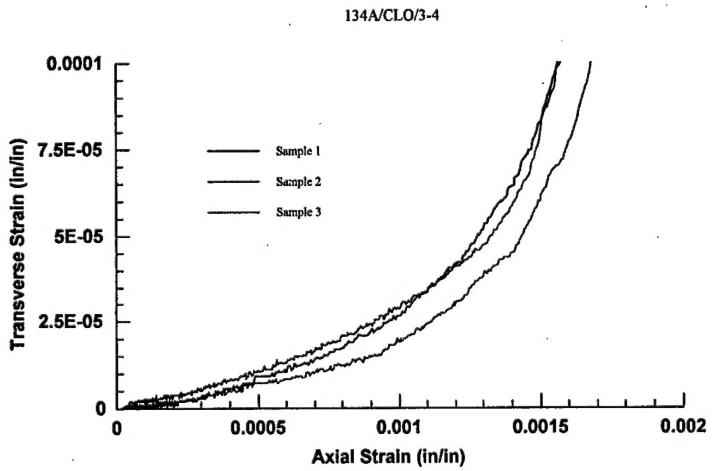

Figure 42 134A/CLO/3-4 composite axial and transverse strains response

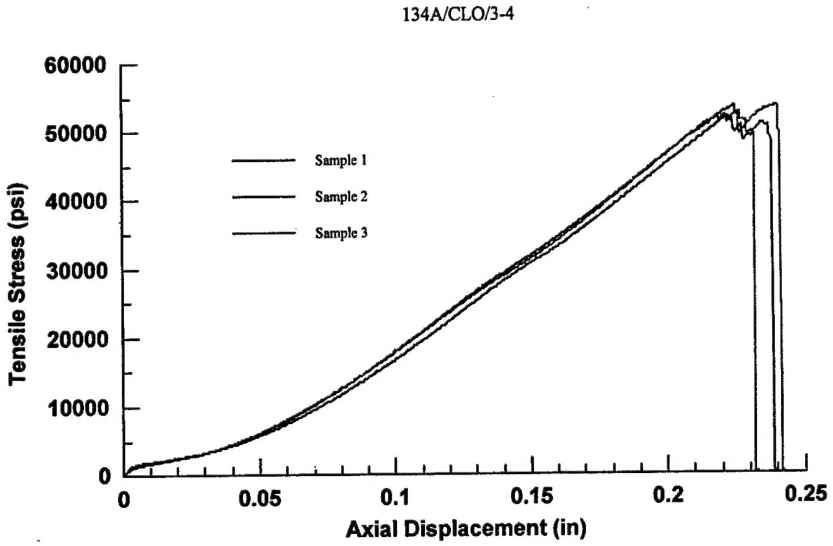

Figure 43 134A/CLO/3-4 composite axial stress-displacement response

Table 11 Comparison of UTS, Elastic Modulus, Poisson's Ratio, and ILSS of the Six Materials in RT and Heat-Aged Conditions

Material	UTS (ksi)	Modulus (msi)	Poisson's Ratio	ILSS (ksi)
CC139-4	46.5	13.0	0.074	2.83
134A/CLO/3-4	53.2	17.0	0.026	1.7
134A/POSS/3-4	51.2	16.8	0.020	1.92
PT30/CLO/5-4	43.4	13.8	0.036	2.09
PTPT30PR24PS1-4	59.2	14.3	0.025	1.94
CC139-3	47.8	12.8	0.111	2.76
PT30/CLO/5-3	33.5	14.7	0.028	1.94
PT30/PR24PS/1-3	60.4	13.9	0.033	1.94

4. SUMMARY AND CONCLUSIONS

Three resin systems (134A phenolic, PT-15 and PT-30 cyanate esters) and three types of nanoparticles (MMT nanoclay, POSS®, and CNF) were selected for this study. The TEM analysis was used to characterize and screen candidates based on their degree of dispersion. Six candidates and one baseline (CC139) carbon/carbon composites were selected to produce prepregs and cured composites. A set of four 12.25- by 12.25- by 0.15-inch CCC panels were fabricated for each candidate and for the baseline materials. Heat-aging of the NCCCs were conducted at 700° and 1,200°F in nitrogen for 24 hrs. and were then exposed to heated-air for 8 hrs. simulating thermo-oxidative conditions. Mechanical properties such as tensile strength, tensile modulus, Poisson's ratio, and interlaminar shear strength were measured and compared with CC139 at room temperature and 1,200°F testing conditions.

The following conclusions were drawn from this study:

1. The TEM analysis has been demonstrated as an effective tool to characterize and screening candidates based on their degree of dispersion.

2. MMT clay, POSS®, and CNF dispersed very well in the PT-30 and PT-15 cyanate ester resins and not in the 134A phenolic resin which made the cyanate ester nanocomposites more desirable than the phenolic nanocomposites. TEM evidence of molecular dispersing of POSS® into PT-15 could not be demonstrated into improved thermo-oxidative stability (less weight loss) due to specimen overexposure or loss.
3. The nanomodified cyanate ester carbon/carbon composites (PT30/PR24PS/1 and PT30/CLO/5) are more thermo-oxidative resistant than the baseline CCC (CC139). The nanomodified phenolic carbon/carbon composites (134A/CLO/3 and 134A/POSS/3) are less thermo-oxidative resistant than the baseline CC139 material.
4. The densities of nanomodified cyanate ester CCC (PT30/PR24PS/1, PT30/CLO/5, and PT15/POSS/5) were higher than the baseline CCC (CC139) while the densities of the nanomodified phenolic CCC (134ACLO/3 and 134A/POSS/3) were lower than CC139.
5. The higher density NCCCs have less weight loss than the lower density phenolic modified NCCC and CC139 which make them more thermo-oxidative resistant.
6. Blisters/delaminations of NCCCs were the result of improper heating cycle of as cured composite part. The use of DSC during cure of cyanate ester resin to determine optimum cure conditions is proposed to reduce or eliminate blisters/delaminations.
7. The ultimate tensile strength of CC139-4, 134A/CLO/3-4, 134A/POSS/3-4, PT30/CLO/5-4, and PT30/PR24PS/1-4 panels at room temperature were 46.5, 53.2, 51.2, 43.4, 59.2 ksi, respectively. Increased in UTS of NCCCs over baseline may be due to nanophase formation.
8. Elastic modulus of CC139-4, 134A/CLO/3-4, 134A/POSS/3-4, PT30/CLO/5-4, and PT30/PR24PS/1-4 were 13.0, 17.0, 16.8, 13.8, and 14.3 msi, respectively. Increased elastic modulus of NCCCs over baseline may be due to nanophase formation.
9. The average Interlaminar shear strength (ILSS) of CC139-4, 134A/CLO/3-4, 134A/POSS/3-4, PT30/CLO/5-4, and PT30/PR24PS/1-4 panels at room temperature were 2.8, 1.7, 1.9, 2.1, and 2.2 ksi, respectively. The heat aged (1,200°F) CC139-3, PT30/CLO/5-3, PT30/PR24PS/1-3 panels lost 3, 9, and 13% of the ILSS, respectively.
10. The PT30/PR24PS-3, -4 specimens had the highest UTS. They exhibited largest maximum failure load (for both RT and 1,200°F heat aged specimens) and then gradually fell off to 75% load until complete fracture. It appears that CNF would enhance the ductility while increasing the ultimate strength.
11. All nanoclay NCCCs were significantly weaker and also had excessive blisters. Nanoclay may hurt the CCC if proper heating cycling is not used in the pyrolysis of the as cured panels. Improved thermal stability surface modified clays with alkyl imidazole surfacing agents and controlled cure (DSC) will eliminate blisters and improve cured panel appearance and performance of nanoclay cyanate ester panels.
12. All the PT-30 materials had micro cracking as well as some blistering, particular the nanoclay specimens which had blister near mid-plane and surface plies
13. A set of PT15/CLO/5-1, PT15/CLO/5-2, PT15/CLO/5-3, and PT15/CLO/5-4 had been fabricated; thermo-oxidative studies and mechanical properties testing are in progress. The results will be reported elsewhere later [7].
14. Microstructure analyses of pre- and post-test NCCC specimens would gain more fundamental understanding of material behavior.

5. REFERENCES

1. K. Shivakumar, F. Abali, R. Sadler, J. McCoy, "Development of Cyanate Ester Based Carbon/Carbon Composites," *Proc. SAMPE 2000 Int'l Symposium*, SAMPE, Covina, CA May 2000, p. 1005-1015.
2. F. Abali, K. Shivakumar, N. Hamidi, and R. Sadler, "An RTM Densification Method of Manufacturing Carbon-Carbon Composites Using PT-30 Resin" manuscript from Shivakumar, 2001.
3. Hitco 134A technical data sheet, Hitco Carbon Composites, Gardena, CA.
4. Hitco CC139 technical data sheet, Hitco Carbon Composites, Gardena, CA.
5. J.H. Koo, H. Stretz, A. Bray, J. Weispfenning, Z.P Luo, and W. Wootan, "Nanocomposite Rocket Ablative Materials: Processing, Characterization, and Performance," *Proc. SAMPE 2003 Int'l Symposium*, SAMPE, Covina, CA, May 2003, p. 1156-1170.
6. J.H. Koo, C.U. Pittman, Jr., K. Liang, H. Cho, L.A. Pilato, Z.P. Luo, G. Pruett, and P. Winzek, "Nanomodified Carbon/Carbon Composites for Intermediate Temperature: Processing and Characterization," *Proc. 35th International SAMPE Technical Conference*, SAMPE, Covina, CA, 2003.
7. J.H. Koo, L.A. Pilato, C.U. Pittman, Jr., N. Shivakumar, P. Winzek, Z.P. Luo, and G. Pruett, "Nanomodified Carbon/Carbon Composites for Intermediate Temperature: Thermal and Mechanical Properties," accepted for presentation at the 49th *International SAMPE Symposium*, Long Beach, CA, May 17-20, 2004.

ACKNOWLEDEMENTS

This work was sponsored by Air Force Office of Scientific Research (AFOSR) under AFOSR Contract No. F49620-02-C-0086 (STTR Phase I) with Dr. Charles Y-C Lee as our Program Manager. The authors would like to thank M. Lake of Applied Sciences, Dr. G. Wissler of 21st Century Polymers, Dr. G. Pruett of Hitco, Dr. J. Lichtenhan of Hybrid Plastics, Dr. S. Das of Lonza, K. Liang and H. Cho of Mississippi State University, Dr. K. Shivakumar of North Carolina A&T State University, Dr. D. Hunter of Southern Clay Products, and Dr. Z.P. Luo of Texas A&M University for supporting the program.